

Mode selectivity of dynamically induced conformation in many-body chain-like bead-spring model

Yoshiyuki Y. Yamaguchi*

*Department of Applied Mathematics and Physics,
Graduate School of Informatics, Kyoto University, Kyoto 606-8501, Japan*

We consider conformation of a chain consisting of beads connected by stiff springs, where the conformation is determined by the bending angles between the consecutive two springs. A conformation is stabilized or destabilized not only by a given bending potential but also the fast spring motion, and stabilization by the spring motion depends on their excited normal modes. This stabilization mechanism has been named the dynamically induced conformation in a previous work on a three-body system. We extend analyses of the dynamically induced conformation in many-body chain-like bead-spring systems. The normal modes of the springs depend on the conformation, and the simple rule of the dynamical stabilization is that the lowest eigenfrequency mode contributes to the stabilization of the conformation. The high the eigenfrequency is, the more the destabilization emerges. We verify theoretical predictions by performing numerical simulations.

I. INTRODUCTION

Conformation has a deep relationship to function as found in isomerization. Maintenance of a conformation requires stability, and the stability is usually associated with landscape of the given potential energy function. We however underline that dynamics also contributes to the stability.

A typical example of the dynamical stabilization is the Kapitza pendulum, which is the inverted pendulum under the uniform gravity [1, 2]. The inverted pendulum is stabilized by applying fast vertical oscillation of the pivot. This highly unintuitive stabilization is applied in a wide variety of fields due to importance of the mechanism [3–19].

In the Kapitza pendulum the stabilization is realized by adding fast motion externally. We stress that the fast oscillation is not necessarily external, and an internal fast oscillation can also stabilize a conformation in an autonomous system. Indeed, in a chain-like bead-spring model consisting of beads connected by stiff springs, the straight conformation is stabilized by fast spring motion, whereas the potential energy function contains only the spring energy and does not depend on the bending angles [20].

The above dynamical stabilization in a bead-spring model is firstly observed in numerical simulations, and then theoretically analyzed in the three-body model [21] with the aids of the multiple-scale analysis [22] and the averaging method [23–25]. A surprising result is that the stability of a conformation depends on the excited normal modes of the springs. Suppose that the system has the equal masses and the identical springs. The straight (the fully bent) conformation is stabilized (destabilized) by the in-phase mode and is destabilized (stabilized) by the antiphase mode. Here, the in-phase (the antiphase) mode is a normal mode of the springs, and is defined as

the two springs expand and contract simultaneously (alternatively). The stabilization is obtained from dynamics of the springs, and the obtained conformation is called the dynamically induced conformation (DIC).

The previous analysis is performed in the three-body model, and several natural questions are induced in many-body systems: Is DIC ubiquitous? How does the stability of a conformation depend on the excited normal modes? Is there a simple rule in the dependence? The aim of this paper is to answer these questions in chain-like bead-spring models.

The present study has another importance in the context of conformational isomerization in flexible molecules. It is experimentally observed in *N*-acetyl-tryptophan methyl amide that population of isomers is modified by exciting vibration in a bond, and the modified population depends on the excited bond [26], whereas the Rice-Ramsperger-Kassel-Marcus theory [27–29] states that the destination is determined statistically. This mode selectivity may have a deep connection with the mode dependence of DIC.

This paper is organized as follows. The chain-like bead-spring model is introduced in Sec. II with the equations of motion. We extract the equations of motion for the slow bending motion in Sec. III. Assuming absence of the bending potential for observing the simplest case, we theoretically exhibit the excited mode dependence of stability with concentrating on one-dimensional conformations, whose bending angles are 0 or π . The theoretical predictions are examined through numerical simulations in Sec. V with applying the Lennard-Jones potential as the bending potential. Finally, Sec. VI is devoted to summary and discussions.

II. MODEL

We consider the N -body chain-like bead-spring model on \mathbb{R}^2 . The model consists of N beads connected by $N - 1$ springs. The i th bead is characterized by the

* yyama@amp.i.kyoto-u.ac.jp

mass $m_i \in (0, \infty)$, the position $\mathbf{r}_i \in \mathbb{R}^2$, and the velocity $\dot{\mathbf{r}}_i = d\mathbf{r}_i/dt \in \mathbb{R}^2$, where $t \in \mathbb{R}$ is the time and \mathbf{r}_i are column vectors. See Fig. 1 for a schematic diagram of the system.

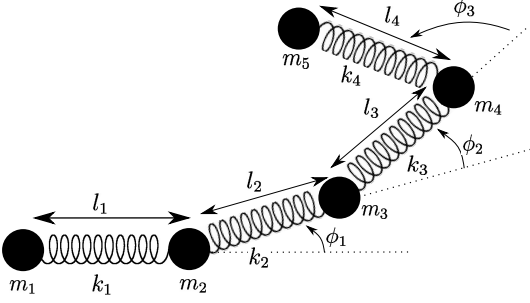


FIG. 1. The bead-spring model on \mathbb{R}^2 . This diagram shows an example of $N = 5$ (five beads connected by four springs).

A. Lagrangian in Cartesian coordinates

The Lagrangian of the system is

$$L(\mathbf{r}, \dot{\mathbf{r}}) = K(\dot{\mathbf{r}}) - V(\mathbf{r}) \quad (1)$$

in the Cartesian coordinates, where

$$\mathbf{r} = \begin{pmatrix} \mathbf{r}_1 \\ \vdots \\ \mathbf{r}_N \end{pmatrix}, \quad \dot{\mathbf{r}} = \begin{pmatrix} \dot{\mathbf{r}}_1 \\ \vdots \\ \dot{\mathbf{r}}_N \end{pmatrix} \in \mathbb{R}^{2N}. \quad (2)$$

The kinetic energy function $K(\dot{\mathbf{r}})$ is

$$K(\dot{\mathbf{r}}) = \frac{1}{2} \sum_{i=1}^N m_i \|\dot{\mathbf{r}}_i\|^2. \quad (3)$$

The potential energy function $V(\mathbf{r})$ consists of the spring potential V_{spring} and the bending potential U_{bend} as

$$V(\mathbf{r}) = V_{\text{spring}}(\mathbf{r}) + U_{\text{bend}}(\mathbf{r}), \quad (4)$$

where we assume that V_{spring} depends on only the lengths of the springs. When we consider a molecule, the spring potential represents stronger bonds, and the bending potential corresponds to weaker bonds. A chain-like model is expressed by the nearest neighbor interactions in the spring potential as

$$V_{\text{spring}}(\mathbf{r}) = \sum_{i=1}^{N-1} V_i(\|\mathbf{r}_{i+1} - \mathbf{r}_i\|). \quad (5)$$

B. Lagrangian in internal coordinates

The system described by the Lagrangian (1) has the two-dimensional translational symmetry. To reduce the

two degrees of freedom, we introduce $2N - 2$ internal coordinates $\mathbf{y} \in \mathbb{R}^{2N-2}$ as

$$\mathbf{y} = \begin{pmatrix} \mathbf{l} \\ \boldsymbol{\phi} \end{pmatrix} \in \mathbb{R}^{2N-2}, \quad \begin{cases} \mathbf{l} = (l_1, \dots, l_{N-1})^T \in \mathbb{R}^{N-1} \\ \boldsymbol{\phi} = (\phi_1, \dots, \phi_{N-1})^T \in \mathbb{R}^{N-1} \end{cases} \quad (6)$$

where the superscript T represents transposition. The internal coordinates play an important role to extract coupling between bending motion and spring motion (see Ref. [30] for instance).

The vector \mathbf{l} contains the lengths of the springs as

$$l_i = \|\mathbf{r}_{i+1} - \mathbf{r}_i\|, \quad (i = 1, \dots, N-1). \quad (7)$$

The Euclidean norm is defined by $\|\mathbf{x}\| = \sqrt{x^2 + y^2}$ for $\mathbf{x} = (x, y) \in \mathbb{R}^2$.

The angle ϕ_i ($i = 1, \dots, N-2$) represents the bending angle between the vectors $\mathbf{r}_{i+2} - \mathbf{r}_{i+1}$ and $\mathbf{r}_{i+1} - \mathbf{r}_i$, and satisfies

$$\cos \phi_i = \frac{(\mathbf{r}_{i+2} - \mathbf{r}_{i+1}) \cdot (\mathbf{r}_{i+1} - \mathbf{r}_i)}{\|\mathbf{r}_{i+2} - \mathbf{r}_{i+1}\| \|\mathbf{r}_{i+1} - \mathbf{r}_i\|}, \quad (i = 1, \dots, N-2) \quad (8)$$

where $\mathbf{x} \cdot \mathbf{y}$ is the Euclidean inner product between \mathbf{x} and \mathbf{y} . The last angle variable ϕ_{N-1} associates to the total angular momentum. The system has the rotational symmetry and ϕ_{N-1} is a cyclic coordinate, but we keep it for later convenience.

Rewriting the kinetic energy in the variables \mathbf{y} and $\dot{\mathbf{y}}$, and assuming that the total angular momentum is zero, we have the Lagrangian

$$L(\mathbf{y}, \dot{\mathbf{y}}) = \frac{1}{2} \sum_{\alpha, \beta=1}^{2N-2} B^{\alpha\beta}(\mathbf{y}) \dot{y}_\alpha \dot{y}_\beta - V(\mathbf{y}). \quad (9)$$

We used the same symbol $V(\mathbf{y})$ for the potential energy function to simplify the notation. The function $B^{\alpha\beta}(\mathbf{y})$ is the (α, β) element of the matrix $\mathbf{B}(\mathbf{y}) \in \text{Mat}(2N-2)$. Here $\text{Mat}(n)$ represents the set of real square matrices of size n . The explicit form of $\mathbf{B}(\mathbf{y})$ is given in Appendix A. Note that an alphabetic index runs from 1 to $N-1$, and a Greek index runs from 1 to $2N-2$.

C. Euler-Lagrange equations

From now on, we adopt the Einstein notation for the sum: We take the sum over an index if it appears twice in a term. The Euler-Lagrange equation for the variable y_α ($\alpha = 1, \dots, 2N-2$) is expressed as

$$B^{\alpha\beta}(\mathbf{y}) \ddot{y}_\beta + D_\alpha^{\beta\gamma}(\mathbf{y}) \dot{y}_\beta \dot{y}_\gamma + \frac{\partial V}{\partial y_\alpha}(\mathbf{y}) = 0 \quad (10)$$

where

$$D_\alpha^{\beta\gamma}(\mathbf{y}) = \frac{\partial B^{\alpha\beta}}{\partial y_\gamma}(\mathbf{y}) - \frac{1}{2} \frac{\partial B^{\beta\gamma}}{\partial y_\alpha}(\mathbf{y}). \quad (11)$$

III. THEORY

This section provides a general theory to derive the equations of motion which describe the slow bending motion. We introduce two assumptions in Sec. III A with a dimensionless small parameter ϵ ($0 < \epsilon \ll 1$). The small parameter induces expansions of the variables \mathbf{y} and t , where the expansion of t follows the multiple-scale analysis. The spring and bending potentials are also expanded in Sec. III B. The slow bending motion is captured in $O(\epsilon^2)$ of the expanded Euler-Lagrange equations as shown in Sec. III C. To eliminate the fast timescale included in $O(\epsilon^2)$, we perform the averaging over the fast timescale in Sec. III D. The averaged equations are not closed due to autonomy of the system, and we will overcome this difficulty by introducing a hypothesis in Sec. III E and the energy conservation law in Sec. III F. Finally, we will obtain closed equations for the slow bending motion in Sec. III G.

The theory can be simplified in the chain-like model with the aid of the explicit form of the spring potential (5). However, we develop the theory as general as possible in this section.

A. Assumptions and expansions of variables

Let $\mathbf{l}_* = (l_{1,*}, \dots, l_{N-1,*})^T$ be the natural length vector of the springs, namely \mathbf{l}_* solves

$$\frac{\partial V_{\text{spring}}}{\partial \mathbf{l}}(\mathbf{l}_*) = \mathbf{0}. \quad (12)$$

We introduce the two assumptions with a small parameter ϵ :

(A1) The amplitudes of the springs are sufficiently small comparing with the natural lengths. The ratio is of $O(\epsilon)$.

(A2) Large bending motion is sufficiently slow than the spring motion. The ratio of the two timescales is of $O(\epsilon)$.

We express these assumptions by the expansions of t , \mathbf{l} , and ϕ as

$$\frac{d}{dt} = \frac{\partial}{\partial t_0} + \epsilon \frac{\partial}{\partial t_1} \quad (13)$$

and

$$\begin{aligned} \mathbf{l}(t_0, t_1) &= \mathbf{l}_* + \epsilon \mathbf{l}^{(1)}(t_0, t_1), \\ \phi(t_0, t_1) &= \phi^{(0)}(t_1) + \epsilon \phi^{(1)}(t_0, t_1), \end{aligned} \quad (14)$$

which is summarized as

$$\mathbf{y}(t_0, t_1) = \mathbf{y}^{(0)}(t_1) + \epsilon \mathbf{y}^{(1)}(t_0, t_1). \quad (15)$$

The two timescales $t_0 = t$ and $t_1 = \epsilon t$ correspond to the fast spring motion and the slow bending motion, respectively. The vector $\mathbf{l}_* = (l_{1,*}, \dots, l_{N-1,*})^T$ is constant.

We are interested in the large and slow motion of the bending angles described by $\phi^{(0)}(t_1)$.

Two remarks are in order. First, the leading order of the expanded equations of motion is of $O(\epsilon)$, since the leading order of the velocities and the accelerations is of $O(\epsilon)$. Second, the velocities \dot{l}_i and $\dot{\phi}_i$ are of the same order of $O(\epsilon)$, and the fastness of motion in the assumption (A2) connotes a short period. Indeed, the distance of a normal mode orbit is of $O(\epsilon)$ and the period is of $O(\epsilon^0)$, while the distance of the large bending motion is of $O(\epsilon^0)$ and the period is of $O(\epsilon^{-1})$.

B. Expansions of the potential function

We also expand the potential functions V_{spring} and U_{bend} into power series of ϵ . The expansions of the two functions are performed in different ways, as a result of Eq. (14).

The spring potential function V_{spring} is expanded around \mathbf{l}_* as

$$V_{\text{spring}}(\mathbf{l}) = V_{\text{spring}}(\mathbf{l}_*) + \frac{1}{2}(\mathbf{l} - \mathbf{l}_*)^T \mathbf{K}_l (\mathbf{l} - \mathbf{l}_*) + O(\epsilon^3), \quad (16)$$

where the (i, j) element K_l^{ij} of the matrix $\mathbf{K}_l \in \text{Mat}(N-1)$ is

$$K_l^{ij} = \frac{\partial^2 V_{\text{spring}}}{\partial l_i \partial l_j}(\mathbf{l}_*), \quad (i, j = 1, \dots, N-1) \quad (17)$$

and \mathbf{K}_l is assumed to be positive definite.

The bending potential U_{bend} can be also expanded around a stationary point ϕ_* if it exists, but this expansion is not useful since $\|\phi - \phi_*\|$ is not necessarily of $O(\epsilon)$. We thus expand U_{bend} by its amplitude as

$$U_{\text{bend}}(\mathbf{y}) = U_{\text{bend}}^{(0)}(\mathbf{y}) + \epsilon U_{\text{bend}}^{(1)}(\mathbf{y}) + \epsilon^2 U_{\text{bend}}^{(2)}(\mathbf{y}) + \dots \quad (18)$$

It is important to note that $U_{\text{bend}}^{(0)}(\mathbf{y})$ and $U_{\text{bend}}^{(1)}(\mathbf{y})$ solely depend on \mathbf{l} with the conditions

$$\frac{\partial U_{\text{bend}}^{(0)}}{\partial \mathbf{l}}(\mathbf{l}_*) = \frac{\partial U_{\text{bend}}^{(1)}}{\partial \mathbf{l}}(\mathbf{l}_*) = \mathbf{0} \quad (19)$$

for satisfying the assumptions (see Appendix B). Integrating them into the spring potential $V_{\text{spring}}(\mathbf{l})$, we may set $U_{\text{bend}}^{(0)}(\mathbf{y}), U_{\text{bend}}^{(1)}(\mathbf{y}) \equiv 0$. The leading order of U_{bend} is hence of $O(\epsilon^2)$, and this ordering is consistent with weaker bonds derived from the bending potential.

C. Expansion of the Euler-Lagrange equations

Substituting Eqs. (13), (14), (16), and (18) into Eq. (10), we have the expanded equations of motion order by order of ϵ . As remarked in the end of Sec. III A, the nontrivial equations of motion start from $O(\epsilon)$.

1. $O(\epsilon)$

The equations of motion in $O(\epsilon)$ is linear and governed by the springs as

$$\frac{\partial^2 \mathbf{y}^{(1)}}{\partial t_0^2} = -\mathbf{X}(\mathbf{y}^{(0)}) \mathbf{y}^{(1)} \quad (20)$$

where

$$\mathbf{X}(\mathbf{y}) = [\mathbf{B}(\mathbf{y})]^{-1} \mathbf{K} \in \text{Mat}(2N - 2) \quad (21)$$

and

$$\mathbf{K} = \begin{pmatrix} \mathbf{K}_l & \mathbf{O} \\ \mathbf{O} & \mathbf{O} \end{pmatrix} \in \text{Mat}(2N - 2). \quad (22)$$

The symbol \mathbf{O} represents the zero matrix. The variables $\phi^{(0)}$ to observe do not appear in $O(\epsilon)$, and we progress to the next order.

2. $O(\epsilon^2)$

In $O(\epsilon^2)$ the equations of motion are

$$\begin{aligned} B^{\alpha\beta}(\mathbf{y}^{(0)}) (\ddot{y}_\beta)^{(2)} + D_\alpha^{\beta\gamma}(\mathbf{y}^{(0)}) (\dot{y}_\beta)^{(1)} (\dot{y}_\gamma)^{(1)} \\ + \frac{\partial B^{\alpha\beta}}{\partial y_\gamma}(\mathbf{y}^{(0)}) (\dot{y}_\beta)^{(1)} y_\gamma^{(1)} + \frac{\partial U_{\text{bend}}^{(2)}}{\partial y_\alpha}(\mathbf{y}^{(0)}) = 0, \end{aligned} \quad (23)$$

where

$$\begin{aligned} (\dot{\mathbf{y}})^{(1)} &= \frac{d\mathbf{y}^{(0)}}{dt_1} + \frac{\partial \mathbf{y}^{(1)}}{\partial t_0}, & (\ddot{\mathbf{y}})^{(1)} &= \frac{\partial^2 \mathbf{y}^{(1)}}{\partial t_0^2}, \\ (\dot{\mathbf{y}})^{(2)} &= \frac{d^2 \mathbf{y}^{(0)}}{dt_1^2} + 2 \frac{\partial^2 \mathbf{y}^{(1)}}{\partial t_0 \partial t_1}. \end{aligned} \quad (24)$$

The vector $(\dot{\mathbf{y}})^{(1)}$ is the first order part of $\dot{\mathbf{y}}$ and $(\dot{\mathbf{y}})^{(1)} \neq d\mathbf{y}^{(1)}/dt$. The variables $\phi^{(0)}$ appear in $(\dot{\mathbf{y}})^{(1)}$ and $(\ddot{\mathbf{y}})^{(2)}$.

D. Averaging

The equations (23) depend on the fast timescale t_0 through $\mathbf{y}^{(1)}$, and we eliminate it by taking the average. The average in the timescale t_0 is defined by

$$\langle \varphi \rangle = \lim_{T \rightarrow \infty} \frac{1}{T} \int_0^T \varphi(t_0) dt_0. \quad (25)$$

The averaged equations are

$$\begin{aligned} B^{\alpha\beta}(\mathbf{y}^{(0)}) \frac{d^2 y_\beta^{(0)}}{dt_1^2} + D_\alpha^{\beta\gamma}(\mathbf{y}^{(0)}) \frac{dy_\beta^{(0)}}{dt_1} \frac{dy_\gamma^{(0)}}{dt_1} \\ + \frac{\partial U_{\text{bend}}^{(2)}}{\partial y_\alpha}(\mathbf{y}^{(0)}) = \mathcal{A}_\alpha, \end{aligned} \quad (26)$$

where the averaged term \mathcal{A}_α is

$$\mathcal{A}_\alpha = \frac{1}{2} \text{Tr} \left[\frac{\partial \mathbf{B}}{\partial y_\alpha}(\mathbf{y}^{(0)}) \mathbf{X}(\mathbf{y}^{(0)}) \langle \mathbf{y}^{(1)} \mathbf{y}^{(1)\text{T}} \rangle \right]. \quad (27)$$

The symbol Tr represents the matrix trace. We used the relation

$$\left\langle \frac{\partial \mathbf{y}^{(1)}}{\partial t_0} \left(\frac{\partial \mathbf{y}^{(1)}}{\partial t_0} \right)^\text{T} \right\rangle = \mathbf{X}(\mathbf{y}^{(0)}) \langle \mathbf{y}^{(1)} \mathbf{y}^{(1)\text{T}} \rangle \quad (28)$$

proven by performing the integration by parts.

The averaged term \mathcal{A}_α depends on the solution $\mathbf{y}^{(1)}$ to Eq. (20), which is obtained by diagonalizing the matrix $\mathbf{X}(\mathbf{y}^{(0)})$ as

$$\mathbf{X}(\mathbf{y}^{(0)}) \mathbf{P}(\mathbf{y}^{(0)}) = \mathbf{P}(\mathbf{y}^{(0)}) \mathbf{\Lambda}(\mathbf{y}^{(0)}). \quad (29)$$

$\mathbf{P} \in \text{Mat}(2N - 2)$ is a diagonalizing matrix, and the diagonal matrix $\mathbf{\Lambda}$ contains the eigenvalues of \mathbf{X} :

$$\mathbf{\Lambda}(\mathbf{y}^{(0)}) = \text{diag}(\lambda_1, \dots, \lambda_{N-1}, 0, \dots, 0) \in \text{Diag}(2N - 2), \quad (30)$$

where the symbol $\text{Diag}(n)$ represents the set of real diagonal matrices. The $N - 1$ zeroeigenvalues come from the fact $\dim(\text{Ker} \mathbf{K}) = N - 1$ in general. We assume that the corresponding $N - 1$ amplitudes of $\mathbf{y}^{(1)}$ are zero. Since the average of the square of a sinusoidal function is $1/2$, we have in general

$$\langle \mathbf{y}^{(1)} \mathbf{y}^{(1)\text{T}} \rangle = \frac{1}{2} \mathbf{P}(\mathbf{y}^{(0)}) \mathbf{W}(t_1)^2 \mathbf{P}(\mathbf{y}^{(0)})^\text{T}, \quad (31)$$

where

$$\mathbf{W}(t_1) = \text{diag}(w_1, \dots, w_{N-1}, 0, \dots, 0) \in \text{Diag}(2N - 2). \quad (32)$$

The matrix \mathbf{W} contains the $N - 1$ nontrivial amplitudes w_i ($i = 1, \dots, N - 1$), which evolve in the slow timescale t_1 through coupling with $\phi^{(0)}(t_1)$, while the initial phases of $\mathbf{y}^{(1)}$ are eliminated by the average.

Summarizing, the averaged term \mathcal{A}_α is modified by Eqs. (29) and (31) to

$$\begin{aligned} \mathcal{A}_\alpha(\mathbf{y}^{(0)}) &= \frac{1}{4} \text{Tr} \left[\mathbf{P}^\text{T} \frac{\partial \mathbf{B}}{\partial y_\alpha} \mathbf{P} \mathbf{\Lambda} \mathbf{W}(t_1)^2 \right], \\ (\alpha &= 1, \dots, 2N - 2). \end{aligned} \quad (33)$$

We can show that

$$\mathcal{A}_1 = \dots = \mathcal{A}_{N-1} = 0. \quad (34)$$

In other words, the averaged terms survive only in the equations for $\phi^{(0)}$. See Appendix C.

E. Hypothesis

We stress that Eq. (26) is not closed, because the averaged term (33) depends on $\mathbf{W}(t_1)$, which nontrivially

evolves in the timescale t_1 . We have to eliminate the $N - 1$ nontrivial amplitudes $w_i(t_1)$ ($i = 1, \dots, N - 1$). To this end, we introduce the hypothesis [21] inspired from the adiabatic invariance:

$$w_i(t_1)^2 = \nu_i w(t_1)^2 \quad (i = 1, \dots, N - 1). \quad (35)$$

This hypothesis supposes that the normal mode energy ratios are constant of time, and reduces the number of unknown variables from $N - 1$ to one, although the averaged term \mathcal{A}_α depends on the constants ν_i ($i = 1, \dots, N - 1$). We arrange the constants in the matrix

$$\mathbf{N} = \text{diag}(\nu_1, \dots, \nu_{N-1}, 0, \dots, 0) \in \text{Diag}(2N - 2), \quad (36)$$

and the amplitude matrix \mathbf{W} is simplified to

$$\mathbf{W}(t_1)^2 = w(t_1)^2 \mathbf{N}. \quad (37)$$

The averaged term \mathcal{A}_α is then modified to

$$\mathcal{A}_\alpha(\mathbf{y}^{(0)}) = \frac{w(t_1)^2}{4} \text{Tr} \left[\mathbf{P}^T \frac{\partial \mathbf{B}}{\partial y_\alpha} \mathbf{P} \Lambda \mathbf{N} \right]. \quad (38)$$

We remark that the numbering of the normal modes is important in the application of the hypothesis, since the eigenvalues of $\mathbf{X}(\mathbf{y}^{(0)})$ depend on the bending angles $\phi^{(0)}$. In $N = 3$, the two springs expand and contract simultaneously (alternatively) in the in-phase mode (the antiphase mode), which has the energy ratio ν_{in} (ν_{anti}). Adopting $\nu_1 = \nu_{\text{in}}$ and $\nu_2 = \nu_{\text{anti}}$, the hypothesis (35) is approximately verified for any value of $\phi^{(0)}$ [21].

However, the global numbering is not trivial in general, because two eigenvalues of $\mathbf{X}(\mathbf{y}^{(0)})$ may cross by varying $\phi^{(0)}$ as shown in Fig. 2. Nevertheless, the hypothesis is approximately valid when the bending motion is not large, since the system is close to the integrable system, Eq. (20), and the mode numbers can be identified in a local region of $\phi^{(0)}$. Consequently, the hypothesis is useful to study stationarity and stability of a conformation. From now on, we locally number the modes in the ascending order of the eigenvalues (see Fig. 2) unless there otherwise stated.

F. Energy conservation

The last unknown variable $w(t_1)$ is eliminated by the energy conservation. Expanding energy E as $E = \epsilon^2 E^{(2)} + \dots$, the leading term is written as

$$E^{(2)} = \frac{1}{2} \text{Tr} \left[\mathbf{B}(\mathbf{y}^{(0)}) (\dot{\mathbf{y}})^{(1)} (\dot{\mathbf{y}})^{(1)T} \right] + U_{\text{bend}}^{(2)}(\mathbf{y}^{(0)}) + \frac{1}{2} \text{Tr} \left[\mathbf{K} \mathbf{y}^{(1)} \mathbf{y}^{(1)T} \right]. \quad (39)$$

Taking the average, we have

$$\begin{aligned} \langle E^{(2)} \rangle &= \frac{1}{2} \text{Tr} \left[\mathbf{B}(\mathbf{y}^{(0)}) \frac{d\mathbf{y}^{(0)}}{dt_1} \left(\frac{d\mathbf{y}^{(0)}}{dt_1} \right)^T \right] + U_{\text{bend}}^{(2)}(\mathbf{y}^{(0)}) \\ &+ \frac{1}{2} \text{Tr} \left[\mathbf{P}^T \mathbf{K} \mathbf{P} \mathbf{W}^2 \right] \end{aligned} \quad (40)$$

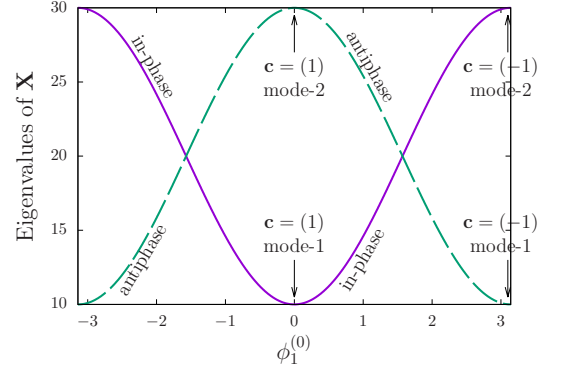


FIG. 2. The two eigenvalues of $\mathbf{X}(\mathbf{y}^{(0)})$, which depend on $\phi_1^{(0)}$ for $N = 3$. The in-phase mode (purple solid line) and the antiphase mode (green dashed line). $m_1 = m_2 = m_3 = m = 1$. $\mathbf{K}_l = k\mathbf{E}$ with $k = 10$, where \mathbf{E} is the unit matrix. The eigenvalues are $(k/m)(2 \mp \cos \phi_1^{(0)})$. The modes are locally numbered in the ascending order of the eigenvalues. The conformation symbol \mathbf{c} is defined in Sec. IV A: $\mathbf{c} = (1)$ represents the straight conformation and $\mathbf{c} = (-1)$ the fully bent conformation.

by the relations (28) and (31). In the right-hand side of Eq. (40), the first line represents the bending energy, and the second line the spring energy.

The hypothesis (36) gives the equality

$$\begin{aligned} w(t_1)^2 \text{Tr} \left[\mathbf{P}^T \mathbf{K} \mathbf{P} \mathbf{N} \right] &= 2 \left[E^{(2)} - U_{\text{bend}}^{(2)}(\mathbf{y}^{(0)}) \right] \\ &- \text{Tr} \left[\mathbf{B}(\mathbf{y}^{(0)}) \frac{d\mathbf{y}^{(0)}}{dt_1} \left(\frac{d\mathbf{y}^{(0)}}{dt_1} \right)^T \right], \end{aligned} \quad (41)$$

where we denoted $\langle E^{(2)} \rangle$ by $E^{(2)}$ for simplicity. Substituting Eq. (41) into Eq. (38), we have the averaged term \mathcal{A}_α as

$$\begin{aligned} \mathcal{A}_\alpha(\mathbf{y}^{(0)}) &= \left\{ \frac{E^{(2)} - U_{\text{bend}}^{(2)}(\mathbf{y}^{(0)})}{2} \right. \\ &\left. - \frac{1}{4} \text{Tr} \left[\mathbf{B}(\mathbf{y}^{(0)}) \frac{d\mathbf{y}^{(0)}}{dt_1} \left(\frac{d\mathbf{y}^{(0)}}{dt_1} \right)^T \right] \right\} \mathcal{S}_\alpha(\mathbf{y}^{(0)}) \end{aligned} \quad (42)$$

where \mathcal{S}_α ($\alpha = 1, \dots, 2N - 2$) are

$$\mathcal{S}_\alpha(\mathbf{y}) = \frac{\text{Tr} \left[\mathbf{P}(\mathbf{y})^T \frac{\partial \mathbf{B}}{\partial y_\alpha}(\mathbf{y}) \mathbf{P}(\mathbf{y}) \Lambda(\mathbf{y}) \mathbf{N} \right]}{\text{Tr} \left[\mathbf{P}(\mathbf{y})^T \mathbf{K} \mathbf{P}(\mathbf{y}) \mathbf{N} \right]}. \quad (43)$$

We can show that

$$\mathcal{S}_1 = \dots = \mathcal{S}_{N-1} = 0. \quad (44)$$

See Appendix C. We remark that in the inside traces of \mathcal{S}_α the size of the matrices can be reduced from $2N - 2$ to $N - 1$ as derived in Appendix C.

We have eliminated the nontrivial unknown variables $w_i(t_1)$ ($i = 1, \dots, N-1$) from the averaged term (42), which depends on only the variables $\phi^{(0)}(t_1)$ and the constants \mathbf{l}_* , \mathbf{N} , and $E^{(2)}$. Therefore, the equations of motion (26) for $\phi^{(0)}$ is now closed, and dynamics depends

on the excited normal modes \mathbf{N} and energy $E^{(2)}$.

G. Final result

Substituting Eq. (42) into Eq. (26), we have

$$B^{\alpha\beta}(\mathbf{y}^{(0)}) \frac{d^2 y_\beta^{(0)}}{dt_1^2} + \left[D_\alpha^{\beta\gamma}(\mathbf{y}^{(0)}) + \frac{1}{4} B^{\beta\gamma}(\mathbf{y}^{(0)}) \mathcal{S}_\alpha(\mathbf{y}^{(0)}) \right] \frac{dy_\beta^{(0)}}{dt_1} \frac{dy_\gamma^{(0)}}{dt_1} + \frac{\partial U_{\text{bend}}^{(2)}(\mathbf{y}^{(0)})}{\partial y_\alpha} - \frac{E^{(2)} - U_{\text{bend}}^{(2)}(\mathbf{y}^{(0)})}{2} \mathcal{S}_\alpha(\mathbf{y}^{(0)}) = 0 \quad (45)$$

for $\alpha = 1, \dots, 2N-2$. The final result for the bending variables $\phi^{(0)}(t_1)$ is

$$\frac{d^2 \phi_i^{(0)}}{dt_1^2} + F_i^{jn}(\mathbf{y}^{(0)}) \frac{d\phi_j^{(0)}}{dt_1} \frac{d\phi_n^{(0)}}{dt_1} + G_i(\mathbf{y}^{(0)}) = 0 \quad (46)$$

for $i = 1, \dots, N-1$. The functions F_i^{jn} and G_i are

$$F_i^{jn}(\mathbf{y}) = \left[B_{\phi\phi}^{-1} \right]^{is} \left(\frac{\partial B_{\phi\phi}^{sj}}{\partial \phi_n} - \frac{1}{2} \frac{\partial B_{\phi\phi}^{jn}}{\partial \phi_s} + \frac{1}{4} \mathcal{T}_s B_{\phi\phi}^{jn} \right) \quad (47)$$

and

$$G_i(\mathbf{y}) = \left[B_{\phi\phi}^{-1} \right]^{is} \left(\frac{\partial U_{\text{bend}}^{(2)}}{\partial \phi_s} - \frac{E^{(2)} - U_{\text{bend}}^{(2)}}{2} \mathcal{T}_s \right). \quad (48)$$

Here, we decomposed the matrix $\mathbf{B} \in \text{Mat}(2N-2)$ into four square submatrices of the size $N-1$ as

$$\mathbf{B}(\mathbf{y}) = \begin{pmatrix} \mathbf{B}_{ll}(\phi) & \mathbf{B}_{l\phi}(\mathbf{y}) \\ \mathbf{B}_{\phi l}(\mathbf{y}) & \mathbf{B}_{\phi\phi}(\mathbf{y}) \end{pmatrix}. \quad (49)$$

See Eq. (A17) for explicit forms of the submatrices. The functions

$$\mathcal{T}_i(\mathbf{y}) = \mathcal{S}_{i+N-1}(\mathbf{y}) = \frac{\text{Tr} \left[\mathbf{P}^T \frac{\partial \mathbf{B}}{\partial \phi_i} \mathbf{P} \Delta \mathbf{N} \right]}{\text{Tr} \left[\mathbf{P}^T \mathbf{K} \mathbf{P} \mathbf{N} \right]} \quad (50)$$

$$(i = 1, \dots, N-1)$$

are introduced to renumber \mathcal{S}_α for avoiding zero-components shown in Eq. (44). It is worth noting that the spring potential V_{spring} is included in the final equations of motion (46) up to the second order, namely only through the matrix \mathbf{K}_l .

IV. DYNAMICALLY INDUCED STABILITY

The equations (46) are rewritten as

$$\frac{d\phi_i^{(0)}}{dt_1} = v_i, \quad \frac{dv_i}{dt_1} = -F_i^{jn}(\mathbf{y}^{(0)}) v_j v_n - G_i(\mathbf{y}^{(0)}), \quad (51)$$

which describe dynamics on the $2N-2$ dimensional space of

$$\Phi = \begin{pmatrix} \phi^{(0)} \\ \mathbf{v} \end{pmatrix} \in \mathbb{R}^{2N-2}, \quad (52)$$

where $\mathbf{v} = (v_1, \dots, v_{N-1})^T$. It is clear that

$$\Phi_* = \begin{pmatrix} \phi_*^{(0)} \\ \mathbf{v}_* \end{pmatrix} : \text{stationary} \iff \begin{cases} \mathbf{G}(\mathbf{y}_*^{(0)}) = \mathbf{0}, \\ \mathbf{v}_* = \mathbf{0}. \end{cases} \quad (53)$$

Stability of a stationary point Φ_* is hence determined by the Jacobian of the vector field $\mathbf{G}(\mathbf{y}_*^{(0)})$, which depends on the averaged terms \mathcal{T}_i and the bending potential $U_{\text{bend}}^{(2)}$.

In this section we concentrate on

$$U_{\text{bend}}^{(2)}(\mathbf{y}) \equiv 0 \quad (54)$$

to clarify the dynamically induced stability by the averaged terms \mathcal{T}_i . According to Eq. (48), $E^{(2)}$ is an overall factor of the function G_i when the bending potential is absent, and stability does not depend on $E^{(2)}$. We come back to the chain-like system

$$\mathbf{K}_l = \text{diag}(k_1, \dots, k_{N-1}) \in \text{Diag}(N-1). \quad (55)$$

Further, we restrict ourselves to the uniform setting

$$m_i = m, \quad k_j = k, \quad l_{j,*} = l_* \quad (1 \leq i \leq N; 1 \leq j \leq N-1) \quad (56)$$

and to the one-dimensional conformations introduced in Sec. IV A.

A. One-dimensional conformations

We introduce the one-dimensional conformations whose set is denoted by

$$\mathcal{C}^1 = \{(\phi_1, \dots, \phi_{N-2}) \mid \phi_i \in \{0, \pi\} \ (i = 1, \dots, N-2)\}. \quad (57)$$

A conformation in \mathcal{C}^1 is stationary as proven in Appendix D. Appearance of the bending potential forbids $\phi_i = \pi$ in

general to avoid collision between beads, but we accept $\phi_i = \pi$ in this section to discuss the simplest case. Later we will perform numerical simulations under appearance of a bending potential which forbids $\phi_i = \pi$.

A conformation in \mathcal{C}^1 is symbolized by a sequence of 1 and -1 : 1 represents the straight joint ($\phi = 0$), and -1 the fully bent joint ($\phi = \pi$). The conformation symbol is denoted by $\mathbf{c} = (c_1, \dots, c_{N-2})$. We identify two symmetric conformations like $(1, -1, -1)$ and $(-1, -1, 1)$, because each of which is mapped to the other by changing the starting end of the chain. All the possible one-dimensional conformations for $N = 5$ are illustrated in Fig. 3 with their conformation symbols.

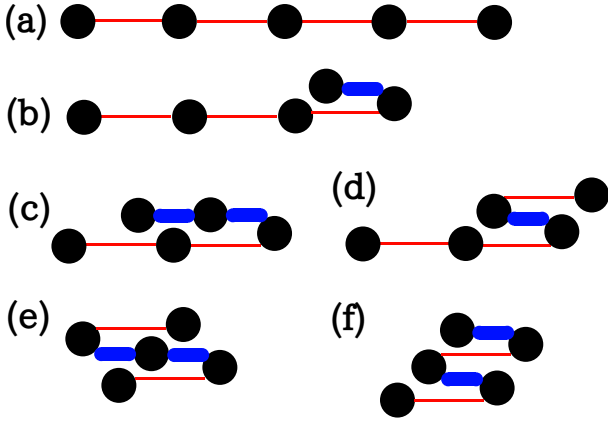


FIG. 3. Illustration of the one-dimensional conformations for $N = 5$. The stabilizing mode is characterized by the two types of bonds: A red thin (a blue thick) bond represents that the spring is longer (shorter) than the natural length. Conformation symbols are (a) $\mathbf{c} = (1, 1, 1)$, (b) $\mathbf{c} = (1, 1, -1)$, (c) $\mathbf{c} = (1, -1, 1)$, (d) $\mathbf{c} = (1, -1, -1)$, (e) $\mathbf{c} = (-1, 1, -1)$, and (f) $\mathbf{c} = (-1, -1, -1)$.

B. Stability

Let the point Φ_* be stationary. Stability of this stationary point is obtained from the eigenvalues of the Jacobian matrix for Eq. (51),

$$\mathbf{J}(\Phi_*) = \begin{pmatrix} \mathbf{O} & \mathbf{E} \\ -DG(\mathbf{y}_*^{(0)}) & \mathbf{O} \end{pmatrix}, \quad (58)$$

where

$$DG = \begin{pmatrix} \frac{\partial G_1}{\partial \phi_1} & \dots & \frac{\partial G_1}{\partial \phi_{N-1}} \\ \vdots & \ddots & \vdots \\ \frac{\partial G_{N-1}}{\partial \phi_1} & \dots & \frac{\partial G_{N-1}}{\partial \phi_{N-1}} \end{pmatrix} \quad (59)$$

is the Jacobian matrix of the vector field $\mathbf{G}(\mathbf{y})$. We do not take the derivatives with respect to the variables \mathbf{l} , because Eq. (51) includes only the constant lengths l_* .

Let us assume that the matrix $DG(\mathbf{y}_*^{(0)})$ is diagonalizable and has the eigenvalues g_1, \dots, g_{N-1} . One eigenvalue, denoted by g_{N-1} , should be zero from the rotational symmetry, and we remove it from the stability criterion. The nontrivial eigenvalues of $\mathbf{J}(\Phi_*)$ are $\pm\sqrt{-g_1}, \dots, \pm\sqrt{-g_{N-2}}$. See Appendix E for a proof and Fig. 4 for a schematic explanation of the relation between the eigenvalues of DG and \mathbf{J} .

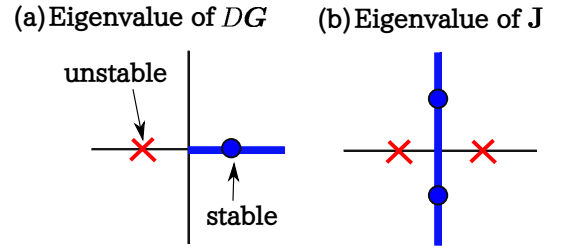


FIG. 4. Eigenvalues of DG and \mathbf{J} on the complex plane. The blue circle in the panel (a) produces the two blue circles in the panel (b), and the same for the red crosses. A conformation is stable if and only if all the eigenvalues are on the blue thick line.

An eigenvalue g_i is called a stable eigenvalue if $g_i \in (0, \infty)$, and a zeroeigenvalue if $g_i = 0$, and an unstable eigenvalue if $g_i \notin [0, \infty)$. The conformation represented by $\phi_*^{(0)}$ is (neutrally) stable [32] if and only if there is no unstable eigenvalue.

C. Mode selectivity of dynamical stabilization

We first excite only one normal mode of the springs: All the diagonal elements of \mathbf{N} are zero except for one element. Stability of the one-dimensional conformations is summarized in Table I with dependency on the excited normal mode, where the normal modes are numbered in the ascending order of the eigenfrequencies around the considering conformation, as mentioned after Eq. (35). Stability is symbolized by S, Z, and U, and the number after S (Z, U) represents the number of the stable (zero, unstable) eigenvalues of DG , whose sum is $N - 2$. The symbol is omitted if the number of corresponding eigenvalues is zero. For instance, the symbol S2U1 represents that the conformation has 2 stable eigenvalues and 1 unstable eigenvalue, and the conformation is unstable.

N	Conformation \mathbf{c}	Stability / Square of eigenfrequency				
		Mode-1	Mode-2	Mode-3	Mode-4	Mode-5
3		S1 / 1	U1 / 3			
	(1)	(+, +)	(+, -)			
	(-1)	(+, -)	(+, +)			
4		S2 / 0.585786	Z2 / 2	U2 / 3.41421		
	(1, 1)	(+, +, +)	(+, 0, -)	(+, -, +)		
	(1, -1)	(+, +, -)	(+, 0, +)	(+, -, -)		
	(-1, -1)	(+, -, +)	(+, 0, -)	(+, +, +)		
5		S3 / 0.381966	S2U1 / 1.38197	S1U2 / 2.61803	U3 / 3.61803	
	(1, 1, 1)	(+, +, +, +)	(+, +, -, -)	(+, -, -, +)	(+, -, +, -)	
	(1, 1, -1)	(+, +, +, -)	(+, +, -, +)	(+, -, -, -)	(+, -, +, +)	
	(1, -1, 1)	(+, +, -, -)	(+, +, +, +)	(+, -, +, -)	(+, -, -, +)	
	(1, -1, -1)	(+, +, -, +)	(+, +, +, -)	(+, -, +, +)	(+, -, -, -)	
	(-1, 1, -1)	(+, -, -, +)	(+, -, +, -)	(+, +, +, +)	(+, +, -, -)	
	(-1, -1, -1)	(+, -, +, -)	(+, -, -, +)	(+, +, -, -)	(+, +, +, +)	
6		S4 / 0.267949	S2Z2 / 1	Z4 / 2	Z2U2 / 3	U4 / 3.73205
	(1, 1, 1, 1)	(+, +, +, +, +)	(+, +, 0, -, -)	(+, 0, -, 0, +)	(+, -, 0, +, -)	(+, -, +, -, +)
	(1, 1, 1, -1)	(+, +, +, +, -)	(+, +, 0, -, +)	(+, 0, -, 0, -)	(+, -, 0, +, +)	(+, -, +, -, -)
	(1, 1, -1, 1)	(+, +, +, -, -)	(+, +, 0, +, +)	(+, 0, -, 0, -)	(+, -, 0, -, +)	(+, -, +, +, -)
	(1, 1, -1, -1)	(+, +, +, -, +)	(+, +, 0, +, -)	(+, 0, -, 0, +)	(+, -, 0, -, -)	(+, -, +, +, +)
	(1, -1, 1, 1)	(+, +, -, -, -)	(+, +, 0, +, +)	(+, 0, +, 0, -)	(+, -, 0, -, +)	(+, -, -, +, -)
	(1, -1, 1, -1)	(+, +, -, -, +)	(+, +, 0, +, -)	(+, 0, +, 0, +)	(+, -, 0, -, -)	(+, -, -, +, +)
	(1, -1, -1, 1)	(+, +, -, +, +)	(+, +, 0, -, -)	(+, 0, +, 0, +)	(+, -, 0, +, -)	(+, -, -, -, +)
	(1, -1, -1, -1)	(+, +, -, +, -)	(+, +, 0, -, +)	(+, 0, +, 0, -)	(+, -, 0, +, +)	(+, -, -, -, -)
	(-1, 1, 1, -1)	(+, -, -, -, +)	(+, -, 0, +, -)	(+, 0, +, 0, +)	(+, +, 0, -, -)	(+, +, -, +, +)
	(-1, 1, -1, -1)	(+, -, -, +, -)	(+, -, 0, -, +)	(+, 0, +, 0, -)	(+, +, 0, +, +)	(+, +, -, -, -)
	(-1, -1, -1, -1)	(+, -, +, -, +)	(+, -, 0, +, -)	(+, 0, -, 0, +)	(+, +, 0, -, -)	(+, +, +, +, +)

TABLE I. Stability of the one-dimensional conformations in the N -body chain-like bead-spring model under the equal masses and the identical springs. The second column from the left represents the conformation symbol \mathbf{c} . The mode number is defined in the ascending order of the eigenfrequencies. Stability of a conformation with a given mode is indicated by S (stable), Z(zero), and U (unstable), and the number after S (Z, U) represents the number of stable (zero, unstable) eigenvalues of $D\mathbf{G}$. After the slash, the value of $(m/k)\omega_j^2$ is shown, where ω_j is the eigenfrequency of the mode. Sequences of +, 0, and - represent the eigenmode symbol \mathbf{s} . See the text for the definitions of \mathbf{c} and \mathbf{s} .

The $(N-1)$ -dimensional eigenvector of a normal mode is characterized by a sequence of +, 0, and -. The symbol + (0, -) represents that the corresponding spring is longer than (equal to, shorter than) the natural length. That is, for $N=3$, the eigenmode (+, +) implies that the two springs are initially longer than the natural length and the mode is the in-phase mode. Similarly, the eigenmode (+, -) represents the antiphase mode. We denote the eigenmode symbol by $\mathbf{s} = (s_1, \dots, s_{N-1})$.

We have two observations in Table I. First, each conformation is stabilized by the lowest eigenfrequency mode of the springs. The number of unstable directions increases as the eigenfrequency gets larger. Second, the stabilizing eigenmode is obtained by pulling the left (right) end of the chain to the left (right) as illustrated in Fig. 3.

Stability analysis can be extended to mixed modes. Analyses for $N=3, 4$ and 5 suggest that the dynamical stabilization is ubiquitous in a larger system having mul-

timode excitation. Indeed, the dynamical stabilization is realized with an approximate probability of 0.8 up to $N=5$, whereas higher eigenfrequency modes contribute to destabilization. See Appendix F.

V. NUMERICAL TESTS

We demonstrate dynamical stabilization and destabilization through numerical simulations of the system under the uniform setting (56) with

$$m = 1, \quad k = 10, \quad l_* = 1. \quad (60)$$

We use the Hamiltonian written in the Cartesian coordinate to use an explicit fourth-order symplectic integrator [31] with the time step $\Delta t = 10^{-3}$. The Hamiltonian

associated with the Lagrangian (1) is

$$H(\mathbf{r}, \mathbf{p}) = \frac{1}{2m} \sum_{i=1}^N \|\mathbf{p}_i\|^2 + V_{\text{spring}}(\mathbf{r}) + U_{\text{bend}}(\mathbf{r}), \quad (61)$$

and the canonical equations of motion are

$$\frac{d\mathbf{r}_i}{dt} = \frac{\partial H}{\partial \mathbf{p}_i}, \quad \frac{d\mathbf{p}_i}{dt} = -\frac{\partial H}{\partial \mathbf{r}_i}, \quad (i = 1, \dots, N). \quad (62)$$

A. System setting

The theory includes the spring potential V_{spring} up to the quadratic order, and we use the linear springs. The spring potential V_{spring} is defined in Eq.(5), and each spring V_i is

$$V_i(\mathbf{r}) = \frac{k}{2} (\|\mathbf{r}_{i+1} - \mathbf{r}_i\| - l_*)^2, \quad (i = 1, \dots, N-1). \quad (63)$$

The bending potential U_{bend} is

$$U_{\text{bend}}(\mathbf{r}) = \sum_{i < j} U_{\text{LJ}}(\|\mathbf{r}_j - \mathbf{r}_i\|), \quad (64)$$

and U_{LJ} is the Lennard-Jones potential

$$U_{\text{LJ}}(r) = 4\epsilon_{\text{LJ}} \left[\left(\frac{\sigma}{r}\right)^{12} - \left(\frac{\sigma}{r}\right)^6 \right]. \quad (65)$$

The parameter ϵ_{LJ} is of $O(\epsilon^2)$, namely

$$\epsilon_{\text{LJ}} = \epsilon_0 \epsilon^2, \quad \epsilon_0 = O(\epsilon^0), \quad (66)$$

to satisfy $U_{\text{bend}} = O(\epsilon^2)$. We fix ϵ_{LJ} and σ as

$$\epsilon_{\text{LJ}} = 10^{-4}, \quad \sigma = 1. \quad (67)$$

We may expect that the main contribution to the bending energy comes from pairs of second nearest beads, since the Lennard-Jones potential does not depend on the bending angles for a pair of nearest beads. For a second nearest pair with the bending angle ϕ , the second-order Lennard-Jones potential is

$$U_{\text{LJ}}^{(2)}(\phi) = 4\epsilon_0 \left\{ \left[\frac{\sigma^2}{2l_*^2(1 + \cos \phi)} \right]^6 - \left[\frac{\sigma^2}{2l_*^2(1 + \cos \phi)} \right]^3 \right\}. \quad (68)$$

It takes the minimum value $-\epsilon_0$ at $\pm\phi_{\text{min}}$, where

$$\phi_{\text{min}} = \left| \cos^{-1} \left[\left(\frac{\sigma}{2^{1/3}l_*} \right)^2 - 1 \right] \right| \simeq 1.94985. \quad (69)$$

See Fig. 5.

It is worth noting that for $N = 3$ we can construct the effective potential [21], which is useful to understand stability of a conformation graphically. Examples are exhibited in Appendix G.

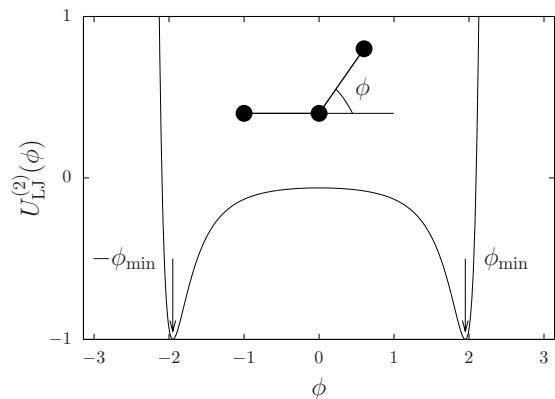


FIG. 5. The second-order Lennard-Jones potential (68). The two arrows mark the minimum points $\pm\phi_{\text{min}}$ (69). $\epsilon_0 = 1$, $\sigma = 1$, and $l_* = 1$. The definition of the bending angle ϕ is schematically represented at the top center.

B. Initial conditions

The initial positions are given in the following three steps. First, we select a reference conformation from \mathcal{C}^1 and put all the beads on the x -axis. Second, we replace the bending angle $\phi = \pi$ with $\phi = \pm\phi_{\text{min}}$ to avoid collision of beads. The possible initial conformations for $N = 5$ are illustrated in Fig. 6. Third, we modify the lengths of the springs from the natural length to $l = l_* + \epsilon l^{(1)}$, where $l^{(1)}$ is determined so as to excite normal modes in a desired manner approximately. Precise settings of the initial positions are described in Appendix H.

The initial values of the momenta are set as follows. For the x -direction, the initial values of the momenta are zero. For the y -direction, they are randomly drawn from the uniform distribution on the interval $[-10^{-3}, 10^{-3}]$ as perturbation to observe stability of the given conformation.

C. Dynamical stabilization and destabilization

We examine dynamical stabilization of high energy conformations. The first example is the straight conformation, which is illustrated in Fig. 6(a). Temporal evolution of $\phi_i(t)$ is exhibited in Fig. 7 by exciting the mode-1 (the stabilization mode) and varying the amplitude ϵ of the mode. For $\epsilon = 0.03$ the bending angles oscillate between the two points $\pm\phi_{\text{min}}$. However, for $\epsilon = 0.04$ which provides larger $E^{(2)}$, the straight conformation is stabilized and the bending angles stay around 0. This observation is consistent with the expression of G_i (48), because larger $E^{(2)}$ enhances contribution from the averaged term \mathcal{T}_s .

The stabilization by the mode-1 is also realized for partially straight conformations. For $N = 5$, temporal evolution of ϕ_i ($i = 1, 2, 3$) are reported in Fig. 8 for

conformations symbolized by $\mathbf{c} = (1, 1, -1)$ [Fig. 6(b)] and $\mathbf{c} = (1, -1, -1)$ [Fig. 6(d)]. The bending angles stay around the initial values.

Finally, we demonstrate destabilization of the bent conformation $\mathbf{c} = (-1, -1, -1)$ [Fig. 6(f)], which is stable if dynamical instability does not kick in. The destabilization is realized by the mode-2 for instance as shown in Fig. 9(a), which is consistent with Table I, although larger spring energy is necessary to destabilize the bent conformation. We stress that the destabilization is not induced only by largeness of energy, because the bent conformation is not destabilized by the mode-1 as shown in Fig. 9(b), while the values of energy are almost equal between the two cases.

VI. SUMMARY

We have studied the dynamically induced conformation (DIC) in N -body chain-like bead-spring models. We have extended a theory, which is developed for $N = 3$ in a previous work [21], to a general N . The theory predicts that the dynamical stability depends on the excited normal modes of the springs and on the value of energy.

As the simplest case we have studied a system without the bending potential to clearly exhibit dynamical effects. Concentrating on the so-called one-dimensional conformations, which are stationary, We have investigated the mode dependent stability up to $N = 6$ under the condition of the equal masses and the identical springs. A simple rule of the mode dependency has been discov-

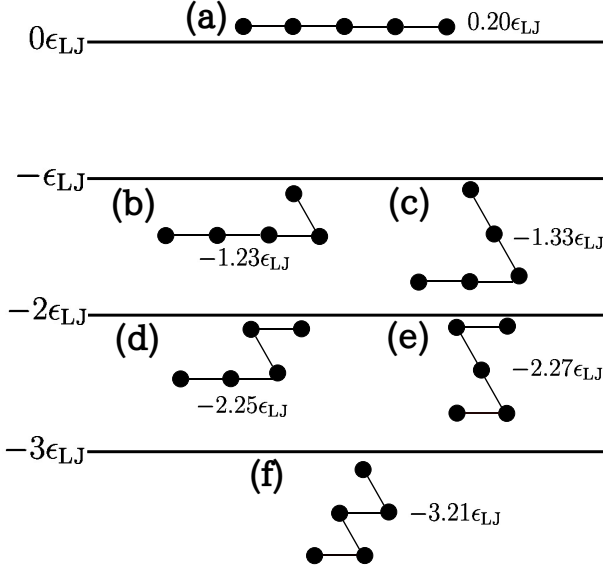


FIG. 6. Illustration of the possible initial conformations and their approximated bending potential energy U_{bend} for $N = 5$. Conformation symbols are (a) $\mathbf{c} = (1, 1, 1)$, (b) $\mathbf{c} = (1, 1, -1)$, (c) $\mathbf{c} = (1, -1, 1)$, (d) $\mathbf{c} = (1, -1, -1)$, (e) $\mathbf{c} = (-1, 1, -1)$, and (f) $\mathbf{c} = (-1, -1, -1)$. The bending angle π has been replaced with $\pm\phi_{\text{min}}$ from Fig. 3.

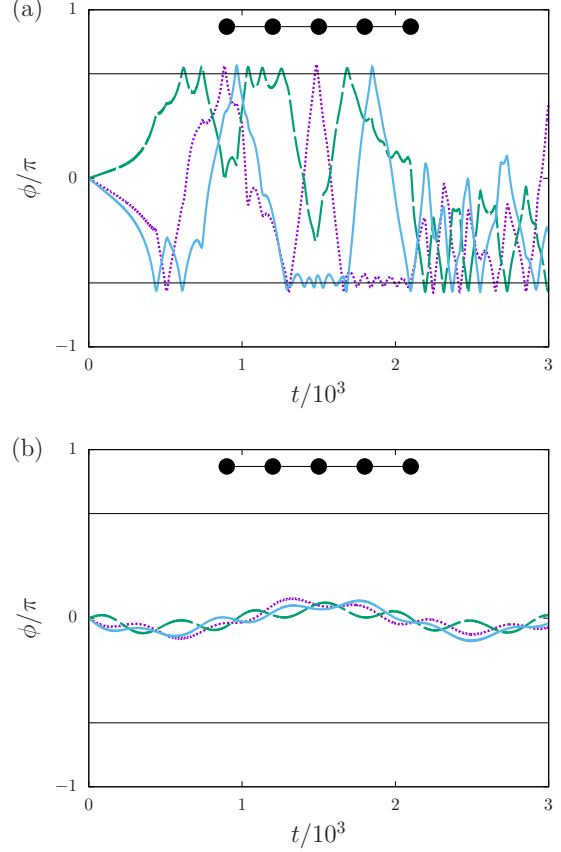


FIG. 7. Temporal evolution of the bending angles. $N = 5$. Conformation is $\mathbf{c} = (1, 1, 1)$, schematically represented at the top of each panel, and the mode-1 is excited. (a) $\epsilon = 0.03$. $E \simeq -0.149\epsilon_{\text{LJ}}$ (b) $\epsilon = 0.04$. $E \simeq 0.070\epsilon_{\text{LJ}}$. $\epsilon_{\text{LJ}} = 10^{-4}$. $\phi_1(t)$ (purple dotted line), $\phi_2(t)$ (green broken line), and $\phi_3(t)$ (blue solid line). Two black horizontal lines are shown at $\pm\phi_{\text{min}}$.

ered: A conformation is stabilized by exciting the lowest eigenfrequency mode, and destabilization emerges as the eigenfrequency of the excited pure normal mode becomes higher.

We stress that DIC is ubiquitous. The theory is also applicable for mixed modes, and the stabilization of a conformation is realized with an approximate probability of 0.8 up to $N = 5$, when we randomly choose a mixed mode. The probability 0.8 is notable, because, among four normal modes in $N = 5$, only one mode contributes to the stabilization and the other three modes contribute to the destabilization. Moreover, the uniform setting of the equal masses and the identical springs is not essential for DIC [21].

The stabilization and destabilization of conformations have been demonstrated numerically in a system having the bending potential consisting of the Lennard-Jones potentials for each pair of beads. As the theory predicts, any conformation can be stabilized by exciting the lowest eigenfrequency mode which depends on the conformation, whereas a straight joint corresponds to the local

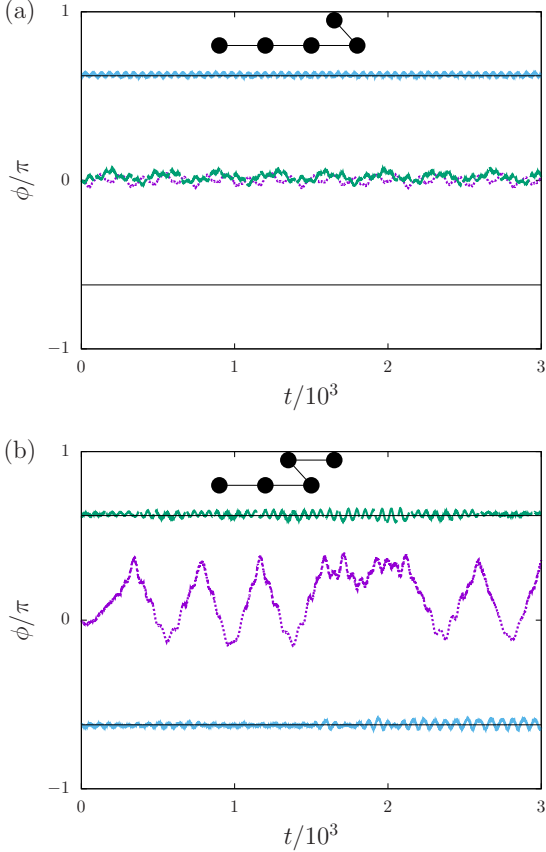


FIG. 8. Temporal evolution of the bending angles. $N = 5$. The mode-1 is excited. (a) Conformation $\mathbf{c} = (1, 1, -1)$, $\epsilon = 0.12$, and $E \simeq 5.22\epsilon_{\text{LJ}}$. (b) Conformation $\mathbf{c} = (1, -1, -1)$, $\epsilon = 0.10$, and $E \simeq 2.45\epsilon_{\text{LJ}}$. $\epsilon_{\text{LJ}} = 10^{-4}$. The conformation is schematically represented at the top of each panel. $\phi_1(t)$ (purple dotted line), $\phi_2(t)$ (green broken line), and $\phi_3(t)$ (blue solid line). Two black horizontal lines are shown at $\pm\phi_{\text{min}}$.

maximum of a Lennard-Jones potential. Destabilization of the fully bend conformation, which corresponds to a local minimum point of the bending potential, has been also demonstrated by exciting a higher eigenfrequency mode.

We note that excitation of a normal mode is a nonequilibrium phenomenon, because the law of equipartition of energy holds among the normal modes in thermal equilibrium. Nevertheless, separation of the two timescales suggests that importance of DIC survives in a long time by the Boltzmann-Jeans conjecture [33–38]. An important message of DIC is that the conformation is not determined by the bending potential only, and we have to input the dynamical (de)stabilization. This message sheds light on a new aspect of conformation and conformation change.

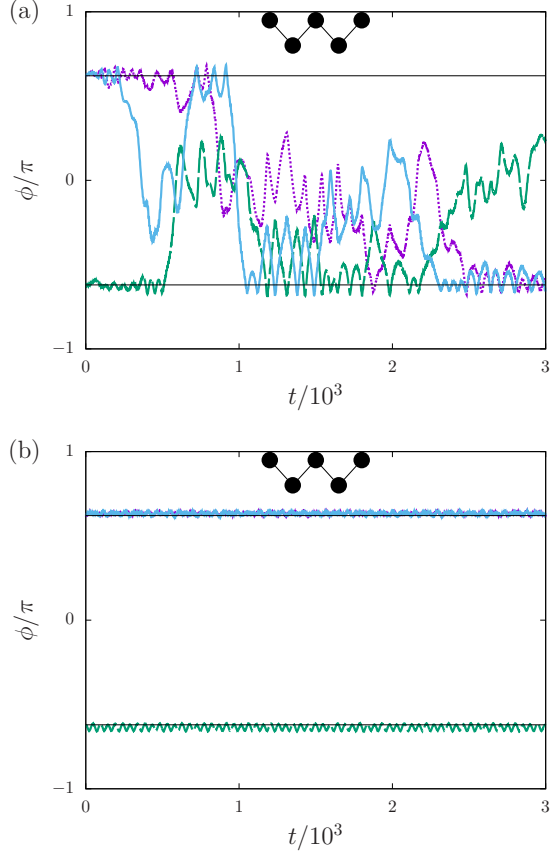


FIG. 9. Excited mode dependence of the bent conformation $\mathbf{c} = (-1, -1, -1)$, schematically represented at the top of each panel. $N = 5$. $\epsilon = 0.16$. (a) The mode-2 is excited and $E \simeq 9.6\epsilon_{\text{LJ}}$. (b) The mode-1 is excited and $E \simeq 10.2\epsilon_{\text{LJ}}$. $\epsilon_{\text{LJ}} = 10^{-4}$. $\phi_1(t)$ (purple dotted line), $\phi_2(t)$ (green broken line), and $\phi_3(t)$ (blue solid line). Two lines are almost collapsed around ϕ_{min} in the panel (b). Two black horizontal lines are shown at $\pm\phi_{\text{min}}$.

ACKNOWLEDGMENTS

The author thanks T. Yanagita, T. Konishi, and M. Toda for valuable discussions. The author acknowledges the support of JSPS KAKENHI Grant Numbers 16K05472 and 21K03402.

Appendix A: Lagrangian in the internal coordinates

We rewrite the Lagrangian Eq. (1) into the internal coordinates through three changes of variables. We mainly consider modifications of the kinetic energy

$$K(\dot{\mathbf{r}}) = \frac{1}{2}\dot{\mathbf{r}}^T \mathbf{M} \dot{\mathbf{r}}, \quad (\text{A1})$$

where

$$\mathbf{M} = \text{diag}(m_1, \dots, m_N) \in \text{Diag}(N) \quad (\text{A2})$$

and the symbol $\text{Diag}(n)$ represents the set of the real diagonal matrices of size n .

The first change of variables is

$$\begin{pmatrix} \mathbf{q}_1 \\ \vdots \\ \mathbf{q}_N \end{pmatrix} = \mathbf{S}_M \begin{pmatrix} \mathbf{r}_1 \\ \vdots \\ \mathbf{r}_N \end{pmatrix} \quad (\text{A3})$$

where the matrix $\mathbf{S}_M \in \text{Mat}(N)$ is

$$\mathbf{S}_M = \begin{pmatrix} -1 & 1 & 0 & \cdots & 0 & 0 \\ 0 & -1 & 1 & \ddots & 0 & 0 \\ 0 & 0 & -1 & \ddots & 0 & 0 \\ \vdots & \ddots & \ddots & \ddots & \ddots & \vdots \\ 0 & 0 & 0 & \cdots & -1 & 1 \\ m_1/M & m_2/M & m_3/M & \cdots & m_{N-1}/M & m_N/M \end{pmatrix} \quad (\text{A4})$$

and

$$M = \text{Tr} \mathbf{M} = \sum_{i=1}^N m_i. \quad (\text{A5})$$

In the new variables \mathbf{q}_i , the kinetic energy K is

$$K(\dot{\mathbf{q}}) = \frac{1}{2} \sum_{i,j=1}^{N-1} A^{ij} \dot{\mathbf{q}}_i \cdot \dot{\mathbf{q}}_j + \frac{\mu}{2} \|\dot{\mathbf{q}}_N\|^2. \quad (\text{A6})$$

The symmetric constant matrix $\mathbf{A} \in \text{Mat}(N-1)$ is defined by

$$\mathbf{S}_M^{-\text{T}} \mathbf{M} \mathbf{S}_M^{-1} = \begin{pmatrix} \mathbf{A} & \mathbf{0} \\ \mathbf{0}^{\text{T}} & n^2 \end{pmatrix}, \quad (\text{A7})$$

where the superscript $-\text{T}$ represents transposition of the inverse matrix and $\mathbf{0}$ is the zero column vector. The variable \mathbf{q}_N is a cyclic coordinate corresponding to the total momentum conservation due to the translational symmetry. We set the total momentum as zero, and we drop the last term of the right-hand side of Eq. (A6).

The second change of variables introduce the polar coordinates. Denoting $\mathbf{q}_i = (q_{xi}, q_{yi}) \in \mathbb{R}^2$, we introduce l_i and θ_i by

$$q_{xi} = l_i \cos \theta_i, \quad q_{yi} = l_i \sin \theta_i. \quad (\text{A8})$$

In the vector form, the polar coordinates are expressed by

$$\mathbf{q}_i = l_i \mathbf{e}_{li}, \quad \dot{\mathbf{q}}_i = \dot{l}_i \mathbf{e}_{li} + l_i \dot{\theta}_i \mathbf{e}_{\theta_i}, \quad (\text{A9})$$

where \mathbf{e}_{li} and \mathbf{e}_{θ_i} are the unit vectors of the radial and the angle directions, respectively. The polar coordinates rewrite the spring potential as $V_{\text{spring}}(\mathbf{l})$, and the kinetic energy K as

$$K = \frac{1}{2} \begin{pmatrix} \dot{\mathbf{l}}^{\text{T}} & \dot{\boldsymbol{\theta}}^{\text{T}} \end{pmatrix} \begin{pmatrix} \mathbf{A}_C(\boldsymbol{\theta}) & \mathbf{A}_S(\boldsymbol{\theta}) \mathbf{L}(\mathbf{l}) \\ -\mathbf{L}(\mathbf{l}) \mathbf{A}_S(\boldsymbol{\theta}) & \mathbf{L}(\mathbf{l}) \mathbf{A}_C(\boldsymbol{\theta}) \mathbf{L}(\mathbf{l}) \end{pmatrix} \begin{pmatrix} \dot{\mathbf{l}} \\ \dot{\boldsymbol{\theta}} \end{pmatrix}. \quad (\text{A10})$$

The diagonal matrix \mathbf{L} is defined by

$$\mathbf{L}(\mathbf{l}) = \text{diag}(l_1, \dots, l_{N-1}) \in \text{Diag}(N-1). \quad (\text{A11})$$

The symmetric matrix \mathbf{A}_C and the antisymmetric matrix \mathbf{A}_S are defined by

$$A_C^{ij}(\boldsymbol{\theta}) = A^{ij} \cos(\theta_i - \theta_j), \quad A_S^{ij}(\boldsymbol{\theta}) = A^{ij} \sin(\theta_i - \theta_j). \quad (\text{A12})$$

The third change of variables introduces the bending angles ϕ as

$$\begin{pmatrix} \phi_1 \\ \vdots \\ \phi_{N-1} \end{pmatrix} = \mathbf{S} \begin{pmatrix} \theta_1 \\ \vdots \\ \theta_{N-1} \end{pmatrix}, \quad (\text{A13})$$

where the constant matrix \mathbf{S} is

$$\mathbf{S} = \begin{pmatrix} -1 & 1 & 0 & \cdots & 0 & 0 \\ 0 & -1 & 1 & \ddots & 0 & 0 \\ 0 & 0 & -1 & \ddots & 0 & 0 \\ \vdots & \ddots & \ddots & \ddots & \ddots & \vdots \\ 0 & 0 & 0 & \cdots & -1 & 1 \\ \frac{1}{N-1} & \frac{1}{N-1} & \frac{1}{N-1} & \cdots & \frac{1}{N-1} & \frac{1}{N-1} \end{pmatrix} \in \text{Mat}(N-1). \quad (\text{A14})$$

The bending angles are from ϕ_1 to ϕ_{N-2} , and we added an additional angle ϕ_{N-1} for later convenience. Performing the change of variables of Eq. (A13), the kinetic energy is modified to

$$K(\mathbf{y}, \dot{\mathbf{y}}) = \frac{1}{2} \dot{\mathbf{y}}^{\text{T}} \mathbf{B}(\mathbf{y}) \dot{\mathbf{y}}, \quad (\text{A15})$$

where the matrix \mathbf{B} is

$$\mathbf{B}(\mathbf{y}) = \begin{pmatrix} \mathbf{B}_{ll}(\boldsymbol{\phi}) & \mathbf{B}_{l\phi}(\mathbf{y}) \\ \mathbf{B}_{\phi l}(\mathbf{y}) & \mathbf{B}_{\phi\phi}(\mathbf{y}) \end{pmatrix} \in \text{Mat}(2N-2) \quad (\text{A16})$$

and the size- $(N-1)$ submatrices are defined by

$$\begin{pmatrix} \mathbf{B}_{ll} & \mathbf{B}_{l\phi} \\ \mathbf{B}_{\phi l} & \mathbf{B}_{\phi\phi} \end{pmatrix} = \begin{pmatrix} \mathbf{A}_C(\boldsymbol{\phi}) & \mathbf{A}_S(\boldsymbol{\phi}) \mathbf{L} \mathbf{S}^{-1} \\ -\mathbf{S}^{-\text{T}} \mathbf{L} \mathbf{A}_S(\boldsymbol{\phi}) & \mathbf{S}^{-\text{T}} \mathbf{L} \mathbf{A}_C(\boldsymbol{\phi}) \mathbf{L} \mathbf{S}^{-1} \end{pmatrix}. \quad (\text{A17})$$

The (i, j) elements of the matrices $\mathbf{A}_C(\boldsymbol{\phi}), \mathbf{A}_S(\boldsymbol{\phi}) \in \text{Mat}(N-1)$ are written respectively as

$$A_C^{ij}(\boldsymbol{\phi}) = A^{ij} \cos \phi_{i,j}, \quad A_S^{ij}(\boldsymbol{\phi}) = A^{ij} \sin \phi_{i,j}, \quad (\text{A18})$$

where

$$\phi_{i,j} = \theta_i - \theta_j = \begin{cases} \phi_{i-1} + \cdots + \phi_j & (i > j), \\ 0 & (i = j), \\ -(\phi_{j-1} + \cdots + \phi_i) & (i < j). \end{cases} \quad (\text{A19})$$

The variable ϕ_{N-1} does not appear in $\mathbf{B}(\mathbf{y})$.

After the three changes of variables, we obtain the Lagrangian in the internal coordinates as Eq. (9). The variable ϕ_{N-1} is a cyclic coordinate corresponding to the rotational symmetry. We keep it for later convenience of computations.

Appendix B: Ordering of the bending potential

Since $\dot{\mathbf{y}}, \ddot{\mathbf{y}} = O(\epsilon)$, the zeroth order equations of motion are

$$\left(\frac{\partial V}{\partial y_\alpha}(\mathbf{y}) \right)^{(0)} = 0, \quad (\alpha = 1, \dots, 2N-2) \quad (\text{B1})$$

which implies

$$\left(\frac{\partial V}{\partial y_\alpha}(\mathbf{y}) \right)^{(0)} = \frac{\partial U_{\text{bend}}^{(0)}}{\partial y_\alpha}(\mathbf{y}^{(0)}) \equiv 0, \quad (\alpha = 1, \dots, 2N-2). \quad (\text{B2})$$

Remembering $\mathbf{y}^{(0)} = (\mathbf{l}_*, \boldsymbol{\phi}^{(0)}(t_1))^T$, we conclude that $U_{\text{bend}}^{(0)}$ has no $\boldsymbol{\phi}$ dependence and $U_{\text{bend}}^{(0)}(\mathbf{l})$ satisfies

$$\frac{\partial U_{\text{bend}}^{(0)}}{\partial \mathbf{l}}(\mathbf{l}_*) = \mathbf{0}. \quad (\text{B3})$$

We can put $U_{\text{bend}}^{(0)}$ as a part of the spring potential $V_{\text{spring}}(\mathbf{l})$ and neglect it. The included $U_{\text{bend}}^{(0)}$ modifies the matrix \mathbf{K} in $O(\epsilon^0)$.

The first order force is

$$\left(\frac{\partial U_{\text{bend}}}{\partial y_\alpha}(\mathbf{y}) \right)^{(1)} = \frac{\partial U_{\text{bend}}^{(1)}}{\partial y_\alpha}(\mathbf{y}^{(0)}). \quad (\text{B4})$$

This force is constant in the fast timescale t_0 . The first order equations of motion are

$$\begin{aligned} \frac{\partial^2}{\partial t_0^2} \begin{pmatrix} \mathbf{l}^{(1)} \\ \boldsymbol{\phi}^{(1)} \end{pmatrix} + \begin{pmatrix} \mathbf{B}_{ll} & \mathbf{B}_{l\phi} \\ \mathbf{B}_{\phi l} & \mathbf{B}_{\phi\phi} \end{pmatrix}^{-1} \begin{pmatrix} \mathbf{K}_l & \mathbf{0} \\ \mathbf{0} & \mathbf{0} \end{pmatrix} \begin{pmatrix} \mathbf{l}^{(1)} \\ \boldsymbol{\phi}^{(1)} \end{pmatrix} \\ = - \begin{pmatrix} \mathbf{B}_{ll} & \mathbf{B}_{l\phi} \\ \mathbf{B}_{\phi l} & \mathbf{B}_{\phi\phi} \end{pmatrix}^{-1} \begin{pmatrix} \partial_l U_{\text{bend}}^{(1)}(\mathbf{y}^{(0)}) \\ \partial_\phi U_{\text{bend}}^{(1)}(\mathbf{y}^{(0)}) \end{pmatrix}. \end{aligned} \quad (\text{B5})$$

Focusing on the second line of the second term in the left-hand side, we find no restoring force in $\boldsymbol{\phi}^{(1)}$. Therefore, if the gradient of $U_{\text{bend}}^{(1)}$ at $\mathbf{y}^{(0)}$ is not zero, secular terms are yielded and they break the perturbation expansion (14). Therefore, $U_{\text{bend}}^{(1)}$ depends on \mathbf{l} only, and satisfies

$$\frac{\partial U_{\text{bend}}^{(1)}}{\partial \mathbf{l}}(\mathbf{l}_*) = \mathbf{0}. \quad (\text{B6})$$

As discussed in $O(\epsilon^0)$, $U_{\text{bend}}^{(1)}(\mathbf{l})$ is also put in the spring potential $V_{\text{spring}}(\mathbf{l})$ and modifies \mathbf{K} in $O(\epsilon)$.

Consequently, the leading order term depending on $\boldsymbol{\phi}$ is $U_{\text{bend}}^{(2)}(\mathbf{y})$. The slow motion of $\boldsymbol{\phi}$ is hence determined by the second-order bending potential, which is the same order as the dynamical effects associated with the averaged term \mathcal{A}_α .

Appendix C: Simplifications

We can simplify expressions of the term \mathcal{A}_α and the spring energy, which help to analyze stability of a stationary state. The idea is to decompose a size- $(2N-2)$ matrix into four half-size submatrices.

1. Decomposition of matrices

We consider the eigenvalue problem

$$\mathbf{X}\mathbf{P} = \mathbf{P}\boldsymbol{\Lambda}, \quad (\text{C1})$$

where $\mathbf{X} = \mathbf{B}^{-1}\mathbf{K}$. The inverse matrix \mathbf{B}^{-1} is obtained as

$$\mathbf{B}^{-1} = \begin{pmatrix} \tilde{\mathbf{B}}_{ll} & \tilde{\mathbf{B}}_{l\phi} \\ \tilde{\mathbf{B}}_{\phi l} & \tilde{\mathbf{B}}_{\phi\phi} \end{pmatrix} \in \text{Mat}(2N-2), \quad (\text{C2})$$

where

$$\begin{aligned} \tilde{\mathbf{B}}_{ll} &= (\mathbf{A}_C + \mathbf{A}_S \mathbf{A}_C^{-1} \mathbf{A}_S)^{-1}, \\ \tilde{\mathbf{B}}_{l\phi} &= -\mathbf{A}_C^{-1} \mathbf{A}_S \tilde{\mathbf{B}}_{ll} \mathbf{L}^{-1} \mathbf{S}^T, \\ \tilde{\mathbf{B}}_{\phi l} &= \mathbf{S} \mathbf{L}^{-1} \mathbf{A}_C^{-1} \mathbf{A}_S \tilde{\mathbf{B}}_{ll}, \\ \tilde{\mathbf{B}}_{\phi\phi} &= \mathbf{S} \mathbf{L}^{-1} \tilde{\mathbf{B}}_{ll} \mathbf{L}^{-1} \mathbf{S}^T. \end{aligned} \quad (\text{C3})$$

See Appendix A for the definitions of the matrices $\mathbf{L}, \mathbf{S}, \mathbf{A}_C$, and \mathbf{A}_S . Note that $\tilde{\mathbf{B}}_{ll} \neq \mathbf{B}_{ll}^{-1}$ in general and that \mathbf{B}^{-1} is symmetric.

The decomposition of \mathbf{B}^{-1} gives

$$\mathbf{X} = \mathbf{B}^{-1}\mathbf{K} = \begin{pmatrix} \tilde{\mathbf{B}}_{ll} \mathbf{K}_l & \mathbf{0} \\ \tilde{\mathbf{B}}_{\phi l} \mathbf{K}_l & \mathbf{0} \end{pmatrix}. \quad (\text{C4})$$

The diagonal matrix $\boldsymbol{\Lambda}$ and a diagonalizing matrix \mathbf{P} are also decomposed as

$$\boldsymbol{\Lambda} = \begin{pmatrix} \boldsymbol{\Lambda}_l & \mathbf{0} \\ \mathbf{0} & \mathbf{0} \end{pmatrix} \in \text{Diag}(2N-2) \quad (\text{C5})$$

and

$$\mathbf{P} = \begin{pmatrix} \mathbf{P}_l & \mathbf{0} \\ \mathbf{P}_\phi & \mathbf{E} \end{pmatrix} \in \text{Mat}(2N-2), \quad (\text{C6})$$

where all the submatrices are of size- $(N-1)$ and \mathbf{E} is the unit matrix. The submatrix \mathbf{P}_l solves the eigenvalue problem

$$\left(\tilde{\mathbf{B}}_{ll} \mathbf{K}_l \right) \mathbf{P}_l = \mathbf{P}_l \boldsymbol{\Lambda}_l, \quad (\text{C7})$$

and the submatrix \mathbf{P}_ϕ is determined from \mathbf{P}_l as

$$\mathbf{P}_\phi = \mathbf{S} \mathbf{L}^{-1} \mathbf{A}_C^{-1} \mathbf{A}_S \mathbf{P}_l. \quad (\text{C8})$$

We further decompose the diagonal matrix \mathbf{W} as

$$\mathbf{W} = \begin{pmatrix} \mathbf{W}_l & \mathbf{0} \\ \mathbf{0} & \mathbf{0} \end{pmatrix} \in \text{Diag}(2N-2). \quad (\text{C9})$$

2. Simplification of the spring energy

The averaged spring energy $\langle E_{\text{spring}} \rangle$ is

$$\langle E_{\text{spring}} \rangle = \frac{1}{2} \text{Tr} \left[\mathbf{P}^T \mathbf{K} \mathbf{P} \mathbf{W}^2 \right] = \frac{1}{2} \text{Tr} \left[\mathbf{P}_l^T \mathbf{K}_l \mathbf{P}_l \mathbf{W}_l^2 \right]. \quad (\text{C10})$$

The matrices of the inside trace are reduced from size $2N - 2$ to size $N - 1$. This expression is modified to

$$\langle E_{\text{spring}} \rangle = \frac{w(t_1)^2}{2} \text{Tr} \left[\mathbf{P}_l^T \mathbf{K}_l \mathbf{P}_l \mathbf{N} \right]. \quad (\text{C11})$$

in the use of the hypothesis (36).

3. Simplification of the averaged terms

Substituting the decomposition of the matrices \mathbf{B} , \mathbf{A} , \mathbf{P} , and \mathbf{W} into Eq. (33) and computing straightforwardly, we have

$$\mathcal{A}_\alpha = \frac{1}{4} \text{Tr} \left[\mathbf{P}_l^T \frac{\partial \tilde{\mathbf{B}}_{ll}^{-1}}{\partial y_\alpha} \mathbf{P}_l \mathbf{A}_l \mathbf{W}_l^2 \right], \quad (\alpha = 1, \dots, 2N - 2). \quad (\text{C12})$$

In the way we used the relation

$$\frac{\partial (\mathbf{A}_C \mathbf{A}_C^{-1})}{\partial y_\alpha} = \mathbf{O} \iff \mathbf{A}_C^{-1} \frac{\partial \mathbf{A}_C}{\partial y_\alpha} \mathbf{A}_C^{-1} = -\frac{\partial \mathbf{A}_C^{-1}}{\partial y_\alpha}. \quad (\text{C13})$$

Similarly, the function \mathcal{S}_α is also simplified to

$$\mathcal{S}_\alpha = \frac{\text{Tr} \left[\mathbf{P}_l^T \frac{\partial \tilde{\mathbf{B}}_{ll}^{-1}}{\partial y_\alpha} \mathbf{P}_l \mathbf{A}_l \mathbf{N}_l \right]}{\text{Tr} \left[\mathbf{P}_l^T \mathbf{K}_l \mathbf{P}_l \mathbf{N}_l \right]}, \quad (\alpha = 1, \dots, 2N - 2) \quad (\text{C14})$$

where

$$\mathbf{N} = \begin{pmatrix} \mathbf{N}_l & \mathbf{O} \\ \mathbf{O} & \mathbf{O} \end{pmatrix}, \quad \mathbf{N}_l = \text{diag}(\nu_1, \dots, \nu_{N-1}). \quad (\text{C15})$$

The expressions (C12) and (C14) prove respectively

$$\mathcal{A}_1 = \dots = \mathcal{A}_{N-1} = 0 \quad (\text{C16})$$

and

$$\mathcal{S}_1 = \dots = \mathcal{S}_{N-1} = 0, \quad (\text{C17})$$

since the matrix $\tilde{\mathbf{B}}_{ll}^{-1}$ does not depend on l .

4. Further simplifications

The average spring energy and the denominator of \mathcal{S}_α are further simplified by choosing a special diagonalizing matrix \mathbf{P}_l , where the matrix \mathbf{P}_l satisfies the eigenvalue

problem (C7). The symmetric matrix \mathbf{K}_l is positive definite, and hence we can define the real symmetric matrix $\sqrt{\mathbf{K}_l}$. Introducing the matrix \mathbf{Q}_l as

$$\mathbf{Q}_l = \sqrt{\mathbf{K}_l} \mathbf{P}_l \in \text{Mat}(N - 1), \quad (\text{C18})$$

the eigenvalue problem is rewritten to

$$\left(\sqrt{\mathbf{K}_l} \tilde{\mathbf{B}}_{ll} \sqrt{\mathbf{K}_l} \right) \mathbf{Q}_l = \mathbf{Q}_l \mathbf{A}_l. \quad (\text{C19})$$

The matrix $\sqrt{\mathbf{K}_l} \tilde{\mathbf{B}}_{ll} \sqrt{\mathbf{K}_l}$ is real symmetric, and hence we can choose $\mathbf{Q}_l \in O(N - 1)$, where $O(N - 1)$ is the set of the orthogonal matrices of size $N - 1$. Using $\mathbf{Q}_l \in O(N - 1)$, we have

$$\mathbf{P}_l^T \mathbf{K}_l \mathbf{P}_l = \mathbf{E}. \quad (\text{C20})$$

This equality simplifies the averaged spring energy to

$$\langle E_{\text{spring}} \rangle = \frac{1}{2} \text{Tr} \mathbf{W}_l^2 = \sum_{i=1}^{N-1} \frac{w_i^2}{2}. \quad (\text{C21})$$

Energy of the mode i is $w_i^2/2$ accordingly. The denominator of \mathcal{S}_α becomes

$$\text{Tr} \left[\mathbf{P}_l^T \mathbf{K}_l \mathbf{P}_l \mathbf{N}_l \right] = \text{Tr} \mathbf{N}_l. \quad (\text{C22})$$

Moreover, we can introduce the normalization of the constants ν_i ($i = 1, \dots, N$) as

$$\text{Tr} \mathbf{N}_l = \sum_{i=1}^{N-1} \nu_i = 1, \quad (\text{C23})$$

since the scale of the spring energy is controlled by $w(t_1)$. Thus, $\langle E_{\text{spring}} \rangle$ is further simplified to

$$\langle E_{\text{spring}} \rangle = \frac{w(t_1)^2}{2} \quad (\text{C24})$$

under the hypothesis (35), and the function \mathcal{S}_α is to

$$\mathcal{S}_\alpha = \text{Tr} \left[\mathbf{P}_l^T \frac{\partial \tilde{\mathbf{B}}_{ll}^{-1}}{\partial y_\alpha} \mathbf{P}_l \mathbf{A}_l \mathbf{N}_l \right], \quad (\text{C25})$$

when we use $\mathbf{Q}_l \in O(N - 1)$ and the normalization (C23).

Appendix D: Stationarity and stability of one-dimensional conformations

We first note that

$$\mathbf{A}_S(\phi \in \mathcal{C}^1) = \frac{\partial \mathbf{A}_C}{\partial \phi_i}(\phi \in \mathcal{C}^1) = \mathbf{O} \quad (i = 1, \dots, N - 1), \quad (\text{D1})$$

because all the elements depend on $\sin \phi_{i,j}$ in \mathbf{A}_S and $\partial \mathbf{A}_C / \partial \phi_i$, and $\sin \phi_{i,j} = 0$ for a conformation belonging to \mathcal{C}^1 . This fact implies that

$$\frac{\partial \tilde{\mathbf{B}}_{ll}^{-1}}{\partial \phi_i}(\phi \in \mathcal{C}^1) = \left[\frac{\partial \mathbf{A}_C}{\partial \phi_i} + \frac{\partial (\mathbf{A}_S \mathbf{A}_C^{-1} \mathbf{A}_S)}{\partial \phi_i} \right]_{\phi \in \mathcal{C}^1} = \mathbf{O} \quad (\text{D2})$$

and

$$\mathcal{T}_i(\phi \in \mathcal{C}^1) = 0 \quad (\text{D3})$$

for $i = 1, \dots, N-1$. Thus, we have $\mathbf{G}(\phi \in \mathcal{C}^1) = \mathbf{0}$ for $U_{\text{bend}}^{(2)} \equiv 0$ from Eq. (48).

Similarly, the Jacobian matrix $D\mathbf{G}$ is simplified as

$$\frac{\partial G_i}{\partial \phi_j}(\phi \in \mathcal{C}^1) = -\frac{E^{(2)}}{2} (B_{\phi\phi}^{-1})^{in} \frac{\text{Tr} [\mathbf{P}_l^T \mathbf{Y}_{nj} \mathbf{P}_l \mathbf{\Lambda}_l \mathbf{N}_l]}{\text{Tr} [\mathbf{P}_l \mathbf{K}_l \mathbf{P}_l \mathbf{N}_l]} \quad (\text{D4})$$

where

$$\mathbf{Y}_{ij} = \frac{\partial^2 \mathbf{A}_C}{\partial \phi_i \partial \phi_j} + \frac{\partial \mathbf{A}_S}{\partial \phi_i} \mathbf{A}_C^{-1} \frac{\partial \mathbf{A}_S}{\partial \phi_j} + \frac{\partial \mathbf{A}_S}{\partial \phi_j} \mathbf{A}_C^{-1} \frac{\partial \mathbf{A}_S}{\partial \phi_i}. \quad (\text{D5})$$

We remark that each of \mathbf{Y}_{ij} ($i, j = 1, \dots, N-1$) is a size- $(N-1)$ matrix. Further, the matrix $\tilde{\mathbf{B}}_{ll}^{-1}$ is also simplified to

$$\tilde{\mathbf{B}}_{ll}^{-1}(\phi \in \mathcal{C}^1) = \mathbf{A}_C(\phi \in \mathcal{C}^1), \quad (\text{D6})$$

and the matrices $\mathbf{\Lambda}_l$ and $\mathbf{Q}_l = \sqrt{\mathbf{K}_l} \mathbf{P}_l$ are obtained from the eigenvalue problem

$$\left(\sqrt{\mathbf{K}_l} \mathbf{A}_C \sqrt{\mathbf{K}_l} \right) \mathbf{Q}_l = \mathbf{Q}_l \mathbf{\Lambda}_l. \quad (\text{D7})$$

Note that we can choose \mathbf{Q}_l from $O(N-1)$.

Appendix E: Eigenvalues of the linearized equations

We consider the eigensystem of the matrix

$$\mathbf{J} = \begin{pmatrix} \mathbf{O} & \mathbf{E} \\ -\mathbf{Z} & \mathbf{O} \end{pmatrix}, \quad (\text{E1})$$

where all the submatrices are of size- n . We assume that \mathbf{Z} is diagonalizable. Suppose that the n eigenvalues of \mathbf{Z} are real, nonzero, and denoted by z_i . The associated n eigenvectors are \mathbf{v}_i satisfying

$$\mathbf{Z} \mathbf{v}_i = z_i \mathbf{v}_i, \quad (i = 1, \dots, n). \quad (\text{E2})$$

It is straightforward to show that the matrix \mathbf{J} has the eigenvalues $\pm \sqrt{-z_i}$ and the associated eigenvectors \mathbf{v}_i^\pm defined by

$$\mathbf{v}_i^\pm = \begin{pmatrix} \mathbf{v}_i \\ \pm \sqrt{-z_i} \mathbf{v}_i \end{pmatrix}. \quad (\text{E3})$$

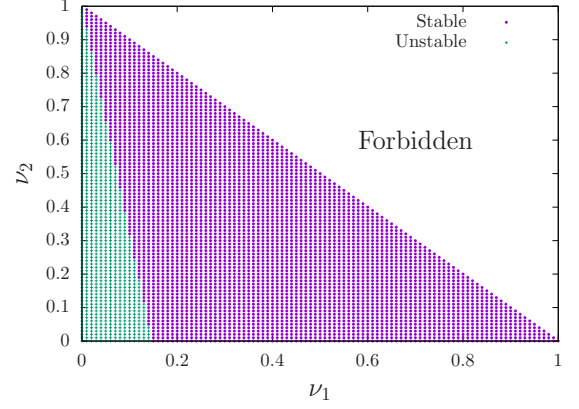


FIG. 10. Stable (purple circles) and unstable (green crosses) regions on the parameter plane (ν_1, ν_2) for $N = 4$. All the one-dimensional conformations share this diagram. The parameter ν_3 is determined by $\nu_3 = 1 - \nu_1 - \nu_2$. The critical point on the line $\nu_2 = 0$ is $\nu_{1c} \simeq 0.1464466$.

Appendix F: Dynamical stability of one-dimensional conformations by mixed modes

We study stability of a one-dimensional conformation with exciting multiple modes under the condition of the equal masses and the identical springs expressed in Eq. (56). The normal mode energy ratios ν_i ($i = 1, \dots, N-1$) are set as

$$\text{Tr } \mathbf{N} = \sum_{i=1}^{N-1} \nu_i = 1, \quad 0 \leq \nu_i \leq 1, \quad (\text{F1})$$

and the number of the free parameters is $N-2$. We compute N dependence of the stable probability $p_s(N)$ with which a considering one-dimensional conformation is stabilized.

A necessary and sufficient condition of the stability for $N = 3$ is

$$\text{the conformation is stable} \iff 1/4 < \nu_1 \leq 1 \quad (\text{F2})$$

for the conformations $\mathbf{c} = (1)$ (straight) and $\mathbf{c} = (-1)$ (bent). The condition implies that the probability is

$$p_s(3) = 0.75. \quad (\text{F3})$$

This stable probability for the two conformations is not a contradiction, because multi-stability of the two conformations is realized in the interval

$$1/4 < \nu_1 < 3/4. \quad (\text{F4})$$

The condition of Eq. (F2) is in agreement with the conclusion reported previously [21]. The agreement suggests that stability can be obtained by the current theory, although it does not reduce the rotational symmetry while the previous theory does.

For $N = 4$, we performed numerical computations of stability at the lattice points $(n_1/100, n_2/100)$ ($n_1, n_2 = 0, \dots, 100$) on the parameter plane (ν_1, ν_2) , where ν_3 is determined from Eq. (F1). The stable and the unstable regions are reported in Fig. 10, and we have the straight line boundary. The critical value ν_{1c} on the line $\nu_2 = 0$ is in the interval $[0.1464466, 0.1464467]$, and the stable probability is

$$p_s(4) \simeq 0.8535. \quad (\text{F5})$$

The stability check on the lattice points is also performed on the parameter space (ν_1, ν_2, ν_3) for $N = 5$. Among all the researched points of 176851, the six conformations are stable at 141019 points. Thus, the stable probability is

$$p_s(5) \simeq 0.7974. \quad (\text{F6})$$

The probabilities $p_s(3)$, $p_s(4)$, and $p_s(5)$ suggest that dynamical stability is important even if the system size is large and multiple modes are excited.

Appendix G: Effective potential for $N = 3$

For $N = 3$, the number of the bending angles is two, and the second bending angle ϕ_2 is not essential, since it is a cyclic coordinate associating with the total angular momentum. Reducing ϕ_2 , we can construct the effective potential, which describes the slow bending motion of ϕ_1 . For simplicity, we denote ϕ_1 by ϕ . The construction is performed in three steps.

First, instead of (ν_1, ν_2) defined in the ascending order of the eigenfrequencies (see the main text), we use $(\nu_{\text{in}}, \nu_{\text{anti}})$, where ν_{in} (ν_{anti}) represents the in-phase (anti-phase) mode energy ratio. This change of ν helps to construct the global effective potential.

Second, we consider the bending potential consisting of the interaction between the first and the third beads only. We set $U_{\text{bend}}^{(2)} = U_{\text{LJ}}^{(2)}$, and the second-order Lennard-Jones potential $U_{\text{LJ}}^{(2)}$ is given in Eq. (68). We set $\epsilon_0 = 1$, $\sigma = 1$, and $l_* = 1$. The graph of $U_{\text{LJ}}^{(2)}$ is reported in Figs. (5) and 11(a).

Third, we construct the effective potential following the previous result [21]. The bending motion is described by the effective Lagrangian

$$L_{\text{eff}} \left(\phi, \frac{d\phi}{dt_1} \right) = \frac{1}{2} M_{\text{eff}}(\phi) \left(\frac{d\phi}{dt_1} \right)^2 - U_{\text{eff}}(\phi). \quad (\text{G1})$$

The effective mass M_{eff} is

$$M_{\text{eff}}(\phi) = \exp \left[2 \int_0^\phi F(\phi') d\phi' \right] \quad (\text{G2})$$

and the effective potential U_{eff} is

$$U_{\text{eff}}(\phi) = \int_0^\phi M_{\text{eff}}(\phi') G(\phi') d\phi'. \quad (\text{G3})$$

The functions F and G are defined by

$$F(\phi) = \frac{1}{2C(\phi)} \frac{\partial C}{\partial \phi}(\phi) + \frac{1}{4} \mathcal{T}(\phi), \quad (\text{G4})$$

and

$$G(\phi) = \frac{1}{C} \left[\frac{dU_{\text{bend}}^{(2)}}{d\phi}(\phi) - \frac{E^{(2)} - U_{\text{bend}}^{(2)}(\phi)}{2} \mathcal{T}(\phi) \right], \quad (\text{G5})$$

where

$$C(\phi) = \frac{ml_*^2}{6} (2 - \cos \phi), \quad (\text{G6})$$

and

$$\mathcal{T}(\phi) = \left(-\frac{\nu_{\text{in}}}{2 - \cos \phi} + \frac{\nu_{\text{anti}}}{2 + \cos \phi} \right) \sin \phi. \quad (\text{G7})$$

We can see that the effective potential depends on the bending potential $U_{\text{bend}}^{(2)}$, the mode energy distribution $(\nu_{\text{in}}, \nu_{\text{anti}})$, and energy $E^{(2)}$. Examples of the effective potential are exhibited in Fig. 11 for three pairs of $(\nu_{\text{in}}, \nu_{\text{anti}})$ with varying $E^{(2)}$. Excitation of the in-phase mode stabilizes the straight conformation ($\phi = 0$), and the antiphase mode enhances the stability around the minimum points $\pm\phi_{\text{min}}$ of the Lennard-Jones potential as $E^{(2)}$ increases.

Appendix H: Initial positions of the beads

We start from a one-dimensional conformation symbolized by $\mathbf{c} = (c_1, \dots, c_{N-2})$. An initial position with the bending potential U_{bend} is prepared by replacing the bending angle $\phi = \pi$ with $\phi = \pm\phi_{\text{min}}$, where ϕ_{min} is a bottom position of the Lennard-Jones potential [see Eq. (69) and Fig. 5], and by approximately exciting normal modes of the one-dimensional conformation \mathbf{c} .

To describe the initial positions of the beads, we introduce the direction vectors \mathbf{d}_i ($i = 1, \dots, N-1$), where

$$\mathbf{d}_1 = (1, 0)^T. \quad (\text{H1})$$

We define \mathbf{d}_i as

$$\mathbf{d}_i = R(\rho_i) \mathbf{d}_{i-1}, \quad (i = 2, \dots, N-1) \quad (\text{H2})$$

where $R(\rho)$ is the rotation matrix of the angle ρ ,

$$R(\rho) = \begin{pmatrix} \cos \rho & -\sin \rho \\ \sin \rho & \cos \rho \end{pmatrix}. \quad (\text{H3})$$

The angles ρ_i are determined as

$$\rho_i = \begin{cases} 0 & (c_i = 1), \\ -\phi_{\text{min}} \prod_{j=1}^i c_j & (c_i = -1), \end{cases} \quad (\text{H4})$$

which replace the bending angle $\phi = \pi$ with $\phi = \pm\phi_{\text{min}}$. Let us denote the initial length of the i th spring by l_i ,

which is determined later. The initial position of the i th bead $\mathbf{r}_{i,0}$ is

$$\mathbf{r}_{1,0} = \mathbf{0}, \quad \mathbf{r}_{2,0} = l_{1,0}\mathbf{d}_1, \quad (\text{H5})$$

and

$$\mathbf{r}_{i,0} = \mathbf{r}_{i-1,0} + l_{i-1,0}\mathbf{d}_{i-1}, \quad (i = 3, \dots, N). \quad (\text{H6})$$

The lengths of the springs are decided to excite normal modes in a desired manner approximately. As discussed in Appendix C4, the matrix \mathbf{P}_l can be constructed as $\mathbf{P}_l = (\sqrt{\mathbf{K}_l})^{-1}\mathbf{Q}_l$, where $\mathbf{Q}_l \in O(N-1)$ solves the eigenvalue problem (C19). For simplicity, we use $\tilde{\mathbf{B}}_l$ defined

for the one-dimensional conformation \mathbf{c} . Since the j th column vector of \mathbf{P}_l represents the j th normal mode of the springs of the one-dimensional conformation \mathbf{c} , we create the vector

$$\hat{\mathbf{p}} = \mathbf{P}_l \begin{pmatrix} \sqrt{\nu_1} \\ \vdots \\ \sqrt{\nu_{N-1}} \end{pmatrix}. \quad (\text{H7})$$

The lengths of the springs are determined as

$$\mathbf{l} = \mathbf{l}_* + \epsilon\hat{\mathbf{p}}. \quad (\text{H8})$$

-
- [1] A. Stephenson, XX. On induced stability, The London, Edinburgh, and Dublin Philosophical Magazine and Journal of Science **15**, 233 (1908).
- [2] P. L. Kapitza, Dynamic stability of a pendulum when its point of suspension vibrates, Soviet Phys. JETP **21**, 588 (1951); Collected papers of P. L. Kapitza, Vol.2, pp.714–737 (1965).
- [3] M. Bukov, L. D’Alessio, and A. Polkovnikov, Universal high-frequency behavior of periodically driven systems: from dynamical stabilization to Floquet engineering, Advances in Physics **64**, 139 (2015).
- [4] M. Grifoni and P. Hänggi, Coherent and incoherent quantum stochastic resonance, Phys. Rev. Lett. **76**, 1611 (1996).
- [5] A. Wickenbrock, P. C. Holz, N. A. Abdul Wahab, P. Phoonthong, D. Cubero, and F. Renzoni, Vibrational mechanics in an optical lattice: Controlling transport via potential renormalization, Phys. Rev. Lett. **108**, 020603 (2012).
- [6] V. N. Chizhevsky, E. Smeu, and G. Giacomelli, Experimental evidence of “vibrational resonance” in an optical system, Phys. Rev. Lett. **91**, 220602 (2003).
- [7] V. N. Chizhevsky, Experimental evidence of vibrational resonance in a multistable system, Phys. Rev. E **89**, 062914 (2014).
- [8] D. Cubero, J. P. Baltanas, and J. Casado-Pascual, High-frequency effects in the Fitzhugh–Nagumo neuron model, Phys. Rev. E **73**, 061102 (2006).
- [9] M. Bordet and S. Morfu, Experimental and numerical study of noise effects in a Fitzhugh–Nagumo system driven by a biharmonic signal, Chaos, Solitons & Fractals **54**, 82 (2013).
- [10] S. H. Weinberg, High frequency stimulation of cardiac myocytes: A theoretical and computational study, Chaos **24**, 043104 (2014).
- [11] M. Uzuntarla, E. Yilmaz, A. Wagemakers, and M. Ozer, Vibrational resonance in a heterogeneous scale free network of neurons, Commun. Nonlinear Sci. Numer. Simulat. **22**, 367 (2015).
- [12] R. H. Buchanan, G. Jameson, and D. Oedjoe, Cyclic migration of bubbles in vertically vibrating liquid columns, Ind. Eng. Chem. Fund. **1**, 82 (1962).
- [13] M. H. I. Baird, Resonant bubbles in a vertically vibrating liquid column, Can. J. Chem. Eng. **41**, 52 (1963).
- [14] G. J. Jameson, The motion of a bubble in a vertically oscillating viscous liquid, Chem. Eng. Sci. **21**, 35 (1966).
- [15] B. Apffel, F. Novkoski, A. Eddi, and E. Fort, Floating under a levitating liquid, Nature **585**, 48 (2020).
- [16] R. E. Bellman, J. Bentsman, and S. M. Meerkov, Vibrational control of nonlinear systems, IEEE Trans. Automat. Contr. **31**, 710 (1986).
- [17] B. Shapiro and B. T. Zinn, High-frequency nonlinear vibrational control, IEEE Trans. Automat. Contr. **42**, 83 (1997).
- [18] M. Borromeo and F. Marchesoni, Artificial sieves for quasimassless particles, Phys. Rev. Lett. **99**, 150605 (2007).
- [19] C. J. Richards, T. J. Smart, P. H. Jones, and D. Cubero, A microscopic Kapitza pendulum, Scientific Reports **8**, 13107 (2018).
- [20] T. Yanagita and T. Konishi, Numerical analysis of new oscillatory mode of bead-spring model, Journal of JSCE A2 **75**, L125 (2019) (in Japanese).
- [21] Y. Y. Yamaguchi, T. Yanagita, T. Konishi, and M. Toda, Dynamically induced conformation depending on excited normal modes of fast oscillation, Phys. Rev. E **105**, 064201 (2022).
- [22] C. M. Bender and S. A. Orszag, Advanced Mathematical Methods for Scientists and Engineers I: Asymptotic Methods and Perturbation Theory (Springer, 1999).
- [23] N. M. Krylov and N. N. Bogoliubov, New Methods of Nonlinear Mechanics in their Application to the Investigation of the Operation of Electronic Generators. I (United Scientific and Technical Press, Moscow, 1934).
- [24] N. M. Krylov and N. N. Bogoliubov, Introduction to Nonlinear Mechanics (Princeton University Press, Princeton, 1947).
- [25] J. Guckenheimer and P. Holmes, Nonlinear Oscillations, Dynamical Systems, and Bifurcations of Vector Fields (Springer-Verlag, New York, 1983).
- [26] B. C. Dian, A. Longarte, T. S. Zwier, Conformational dynamics in a dipeptide after single-mode vibrational excitation, Nature **296**, 2369 (2002).
- [27] O. K. Rice and H. C. Ramsperger, Theories of unimolecular gas reactions at low pressures, J. Am. Chem. Soc. **49**, 1617 (1927).
- [28] L. S. Kassel, Studies in homogeneous gas reactions I, J. Phys. Chem. **32**, 225 (1928).
- [29] R. A. Marcus, Unimolecular dissociations and free radical recombination reactions, J. Chem. Phys. **20**, 359 (1952).

- [30] T. Yanao, W. S. Koon, J. E. Marsden, and I. G. Kevrekidis, Gyration-radius dynamics in structural transitions of atomic clusters, *J. Chem. Phys.* **126**, 124102 (2007).
- [31] H. Yoshida, Construction of higher order symplectic integrators, *Phys. Lett. A* **190**, 262 (1990).
- [32] D. D. Holm, J. E. Marsden, T. Ratiu, and A. Weinstein, Nonlinear stability of fluid and plasma equilibria, *Phys. Rep.* **123**, 1 (1985).
- [33] L. Boltzmann, On certain questions of the theory of gases, *Nature* **51**, 413 (1895).
- [34] J. H. Jeans, On the vibrations set up in molecules by collisions, *Philos. Mag.* **6**, 279 (1903).
- [35] J. H. Jeans, XI. On the partition of energy between matter and aether, *Philos. Mag.* **10**, 91 (1905).
- [36] L. Landau and E. Teller, On the theory of sound dispersion, *Physik. Z. Sowjetaunion* **10**, 34 (1936), in *Collected Papers of L. D. Landau*, edited by D. Ter Haar (Pergamon Press, Oxford, 1965), pp. 147–153.
- [37] G. Benettin, L. Galgani, and A. Giorgilli, Realization of holonomic constraints and freezing of high-frequency degrees of freedom in the light of classical perturbation-theory. Part II, *Commun. Math. Phys.* **121**, 557 (1989).
- [38] O. Baldan and G. Benettin, Classical “freezing” of fast rotations. A numerical test of the Boltzmann-Jeans conjecture, *J. Stat. Phys.* **62**, 201 (1991).

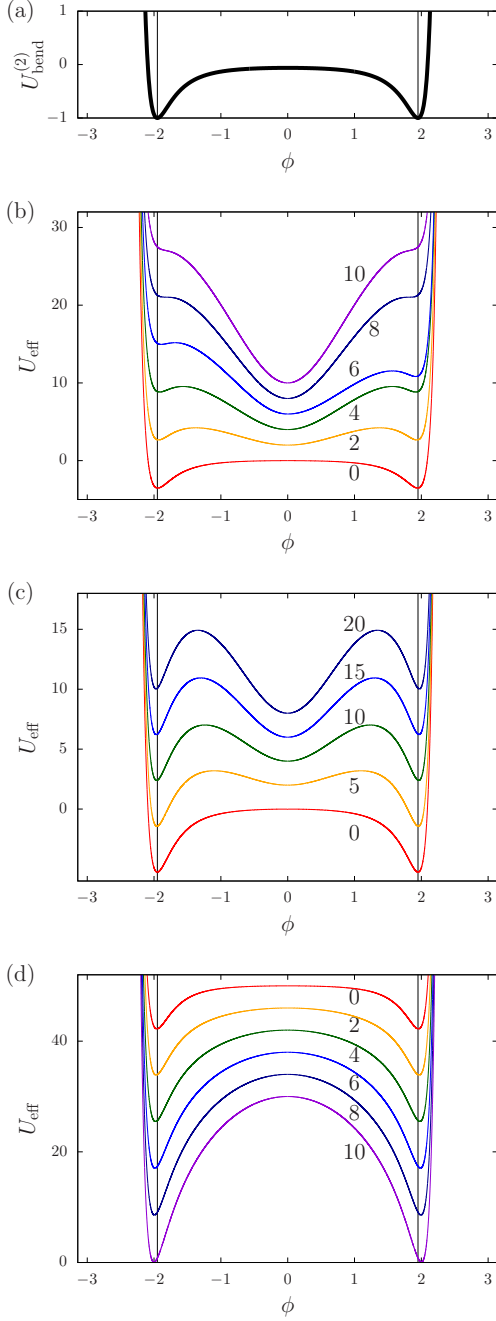


FIG. 11. (a) The Lennard-Jones potential $U_{\text{LJ}}^{(2)}$ as a function of the bending angle ϕ . (b) The effective potential $U_{\text{eff}}(\phi)$ with $(\nu_{\text{in}}, \nu_{\text{anti}}) = (1, 0)$. (c) The effective potential $U_{\text{eff}}(\phi)$ with $(\nu_{\text{in}}, \nu_{\text{anti}}) = (1/2, 1/2)$. (d) The effective potential $U_{\text{eff}}(\phi)$ with $(\nu_{\text{in}}, \nu_{\text{anti}}) = (0, 1)$. The numbers in the panels (b)-(d) represent the values of $E^{(2)}$. $N = 3$, $\epsilon_0 = 1$, $\sigma = 1$, and $l_* = 1$. Graphs are vertically shifted for a graphical reason. The two vertical lines in each panel mark the minimum points $\pm\phi_{\text{min}}$ of the Lennard-Jones potential.